Assessing the function of chromatin modifying enzymes in medulloblastoma

by

Tolga Lokumcu

A Thesis Submitted to the
Graduate School of Engineering
in Partial Fulfillment of the Requirements for
the Degree of
Master of Science
in
Biomedical Sciences and Engineering

Koc University

July 2017

Koc University

Graduate School of Sciences and Engineering

This is to certify that I have examined this copy of a master's thesis by

Tolga Lokumcu

and have found that it is complete and satisfactory in all respects,
and that any and all revisions required by the final
examining committee have been made.

Committee Members:

_____

Tuğba Bağcı-Önder, Ph.D. (Advisor)

_____

Tamer Önder, Ph.D.

_____

Tolga Emre, Ph.D.

Date: _____

ABSTRACT

Medulloblastoma is the most common pediatric brain cancer and it consists of four main molecular subgroups, which are Wingless (WNT), Sonic Hedgehog (SHH), Group 3 and Group 4. These subgroups have different transcriptional, cytogenetic and mutational spectra, making medulloblastoma a complex disease. Current therapy protocols for medulloblastoma include surgical resection, craniospinal irradiation and chemotherapy. Although current treatments result in high overall survival, many survivors experience severe neurological disorders. Therefore, targeted and more efficient therapies are necessary for the treatment of medulloblastoma.

Genomic studies revealed that several chromatin modifying enzymes (CMEs) such as histone methyltransferases (HMTs), histone demethylases (HDMs), histone acetyltransferases (HATs) and histone deacetylases (HDACs) are mutated and/or differentially expressed in medulloblastoma. However, the roles of CMEs in the initiation and progression of medulloblastomas are ill-defined. To this end, we mainly focused on the epigenetics of medulloblastoma to develop novel and more effective therapeutic options.

Firstly, we investigate the roles of chromatin modifiers in medulloblastoma by utilizing a chemical library targeting different chromatin modifying enzymes. Our screen revealed some potential inhibitors, namely GSK-J4, IOX-1, Belinostat, Vorinostat, 5-Azacytidine, ML324, SGC0946, Trichostatin A and Chaetocin, that induced cell death in medulloblastoma cells significantly. To investigate whether these drugs are specific to cancer cells, we tested selected drugs in a dose-dependent manner in non-malignant BJ Fibroblasts and revealed that they were relatively non-toxic to normal cells. Since the roles of histone demethylases are barely defined in medulloblastoma, we focused on KDM6A and KDM6B, which are targets of GSK-J4 and IOX-1. To this end, we targeted KDM6A and KDM6B by shRNAs and examined whether their loss changed the growth rate medulloblastoma cells. However, we did not observe any changes in the proliferation rate of MB cells upon KDM6A and/or KDM6B loss.

Although many medulloblastoma tumors respond to chemotherapy well, there are still many medulloblastoma patients who do not respond to standard of care chemotherapy. As it has been identified that many chromatin modifiers are mutated and/or differentially expressed in the most aggressive and metastatic subgroups (Group 3 and Group 4), we speculated whether chromatin modifiers play role in resistance of medulloblastoma cells to chemotherapeutic agents. From those, vincristine is the main chemotherapeutic agent used in different treatment protocols, we decided to establish a vincristine-resistant medulloblastoma cell line by dose-escalation method to elucidate the function of CMEs in therapy resistance. We performed another drug screen in parental and newly established vincristine-resistant cells

and identified that 8 different HDAC inhibitors (Trichostatin A, Rocilinostat, CXD101, Tubastatin A HCl, Belinostat, Romidepsin, PCI-24781 and Mocetinostat), 2 histone demethylase inhibitors (IOX-1 and KDOBA67), 2 kinase inhibitors (5-Iodotubercidin, SGI-1776), MAZ1805 (Halofuginol) and MAZ1392 induced cell death both in parental and vincristine-resistant cells significantly. Besides, we performed combination treatment with epigenetic drugs and vincristine and discovered that A-395, CBP/BRD4, GSK-J5, GSK343, GSK864, LLY-507, OF-1, SGC-CBP30, SRT1720 and UNC2400 induced cell death of resistant populations when they were combined with vincristine.

ÖZETÇE

Medulloblastoma en sık görülen pediatrik beyin kanseridir. Wingless (WNT), Sonic Hedgehog (SHH), Grup 3 ve Grup 4 olmak üzere dört ana alt gruptan oluşur. Bu alt grupların farklı transkripsiyonel, sitogenetik ve mutasyonel spektrumları vardır. Bu sebeple medulloblastoma karmaşık bir beyin kanseri türüdür. Medulloblastoma için güncel tedavi protokolleri arasında cerrahi operasyon, beyin-omurilik ışınlaması ve kemoterapi bulunmaktadır. Günümüzdeki tedaviler yüksek sağkalım ile sonuçlansa dahi, hayatta kalan birçok hasta ciddi nörolojik rahatsızlıklar yaşamaktadır. Bu nedenle, medulloblastoma tedavisinde güncel ve daha etkili tedaviler gerekmektedir.

Genomik çalışmalar, histon metil transferazlar (HMT), histon demetilazlar (HDM), histon asetiltransferazlar (HATs) ve histon deasetilazlar (HDAC) gibi çeşitli kromatin değiştirici enzimlerin medulloblastomada mutasyona uğramış ve/veya farklı olarak eksprese edildiğini ortaya koymuştur. Bununla birlikte, medulloblastomaların oluşmasında ve ilerlemesinde kromatin değiştirici enzimlerin rolleri detaylıca çalışılmamıştır. Bu amaçla, yeni ve daha etkili tedavi seçenekleri geliştirmek için medulloblastoma epigenetiği üzerine odaklandık.

Öncelikle, farklı kromatin değiştirici enzimleri hedef alan bir kimyasal kitaplık kullanarak medulloblastomadaki kromatin değiştirici enzimlerin görevlerini inceledik. İlaç taramamız, medulloblastoma hücrelerinde hücre ölümünü belirgin şekilde tetikleyen GSK-J4, IOX-1, Belinostat, Vorinostat, 5-Azasitidine, ML324, SGC0946, Trichostatin A ve Chaetocin gibi bazı potansiyel inhibitörleri ortaya koydu. Bu ilaçların kanser hücrelerine özgü olup olmadığını araştırmak için, seçilmiş ilaçları malign olmayan BJ Fibroblast hücre hattında da doza bağımlı bir şekilde test ettik. Seçilmiş ilaçların kanser hücrelerine kıyasla normal hücrelerde nispeten daha az hücre ölümüne neden olduklarını belirledik. Histon demetilazların medulloblastoma üzerindeki rolleri açıkça bilinmediğinden, öncelikli olarak GSK-J4 ve IOX-1'ın bloke ettiği enzimler olan histone demetilaz 6A ve 6B'ye odaklandık. Histon demetilaz 6A ve 6B gen ifadelerinin shRNA ile baskılanmasının hücrelerin bölünmesi üzerindeki etkisini araştırdık fakat bu baskılamanın medulloblastoma hücre büyümesi üzerinde bir etki yaratmadığı gözlemledik.

Birçok medulloblastoma tümörü kemoterapiye iyi yanıt verse bile, standart olarak uygulanan kemoterapiye cevap vermeyen çok sayıda medulloblastoma hastası bulunmaktadır. En agresif ve metastatik medulloblastoma alt gruplarında (Grup 3 ve Grup 4) birçok kromatin değiştiricisinin mutasyona uğramış ve/veya farklı şekilde eksprese edildiği tespit edilmiştir. Bu sebeple bu çalışmada kromatin değiştiricilerin medulloblastoma hücrelerinin kemoterapötik ajanlara direncindeki rollerini araştırdık. Vincristine medulloblastoma terapisinde en sık kullanılan kemoterapötik ilaçlardan biridir. Vincristine tedavisine karşı oluşan dirençte, kromatin değiştirici enzimlerin işlevlerini aydınlatmak için doz

arttırma yöntemi ile Vincristine dirençli bir medulloblastoma hücre hattı oluşturmaya karar verdik. Vincristine duyarlı ve dirençli hücrelerde bir başka ilaç taraması yaptık ve 8 farklı histon deasetilaz inhibitörünün (Trichostatin A, Rocilinostat, CXD101, Tubastatin A HC1, Belinostat, Romidepsin, PCI-24781 ve Mocetinostat), 2 histone demetilaz inhibitörünün (IOX-1 ve KDOBA67), 2 kinaz inhibitörünün (5- Iodotubercidin, SGI-1776), MAZ1805 (Halofuginol) ve MAZ1392'nin hem Vincristine duyarlı hem de dirençli hücrelerde hücre ölümünü tetiklediğini gözlemledik. Ayrıca, epigenetik enzimleri bloke eden ilaçlar ile vincristinin birlikte verildiği durumlarda, A-395, CBP/BRD4, GSK-J5, GSK343, GSK864, LLY-507, OF-1, SGC-CBP30, SRT1720 ve UNC2400'in vincristine dirençli hücrelerin ölümünü indüklediğini keşfettik.

ACKNOWLEDGMENTS

Firstly, I would like to express my gratitude to my thesis advisor Dr. Tuğba Bağcı Önder for her guidance, support and encouragement throughout my master. I am sincerely grateful to her for giving me friendly environment during this master project.

Secondly, I would like to thank Dr. Nathan Lack and Dr. Tamer Önder for their advice and support on my project. I owe special thanks to Dr. Tamer Önder and Dr. Tolga Emre for being in my thesis committee.

Also, I would like to thank Dr. Hakan Sedat Orer for critical discussions about my research project and his help during my PhD applications.

I also express my warm thanks to the members of TBO laboratory; Filiz Şenbabaoğlu, Ahmet Cingöz, Alişan Kayabölen, Fidan Şeker, Ezgi Özyerli, İlknur Sur, Nastaran Langarizadeh and Seher Emreoğlu for their friendship. Also, I would like to express my special thanks to Filiz Şenbabaoğlu for her endless support during my master project.

Last but not the least, I wish to thank my parents and sisters for their love and unfailing support throughout my life.

Table of Contents

List of tables

List of figures

Nomenclature

ABC	ATP-binding cassette
BCOR	BCL6 co-repressor
BCRP	breast cancer resistance protein
CDK6	Cyclin-dependent kinase 6
CGNPs	cerebellar granule neuron precursors
CMEs	Chromatin modifying enzymes
CREBBP	CREB Binding Protein
CSI	craniospinal radiation
CTDNEP1	CTD nuclear envelope phosphatase 1
CTNNB1	β-catenin
DDX3X	DEAD-Box Helicase 3, X-Linked
DNMTs	DNA methyltransferases
EMT	epithelial–mesenchymal transition
GLI2	GLI family zinc finger 2
H3K27me3	Histone 3 Lysine 27 trimethyl
H3K4me3	Histone 3 Lysine 4 trimethyl
HATs	Histone acetyltransferases
HDACs	histone deacetylases
HMTs	Histone methyltransferases
KDM6A	lysine-specific demethylase 6A
KDM6B	lysine-specific demethylase 6B
KMT2D	lysine-specific methyltransferase 2D
LDB1	LIM domain binding 1
MB	Medulloblastoma
MDR	multi-drug resistance

MDR1	multi-drug resistance protein 1
MLL2	mixed lineage leukemia 2
MLL3	mixed lineage leukemia 3
MRI	Magnetic resonance imaging
MRP1	MDR-associated protein 1
OTX2	orthodenticle homeobox 2
PITCH1	patched 1
RT	radiation therapy
SETD2	SET domain containing 2
SHH	Sonic hedgehog
SMO	Smoothened
SUFU	Suppressor of Fused Homolog
TCF4	transcription factor 4
WNT	Wingless

Chapter 1

Review of the Literature

Medulloblastoma

Medulloblastoma is the most common pediatric brain cancer and it consists of four main molecular subgroups, which are Wingless (WNT), Sonic Hedgehog (SHH), Group 3 and Group 4[1,2]. In 2016, World Health Organization revised medulloblastoma subgroups as WNT-activated, SHH-activated and TP53-mutant, SHH-activated TP53-wildtype, and non-WNT/non-SHH Group 3 and Group 4 medulloblastomas[3]. These subgroups have different transcriptional, cytogenetic and mutational spectra, meaning that targeted therapies are necessary for efficient treatment of medulloblastoma[4]. Current therapy protocols for medulloblastoma include surgical resection, craniospinal irradiation and chemotherapy[5–7]. Although current treatments result in high overall survival, many survivors experience intellectual and neurological disorders[8–10].

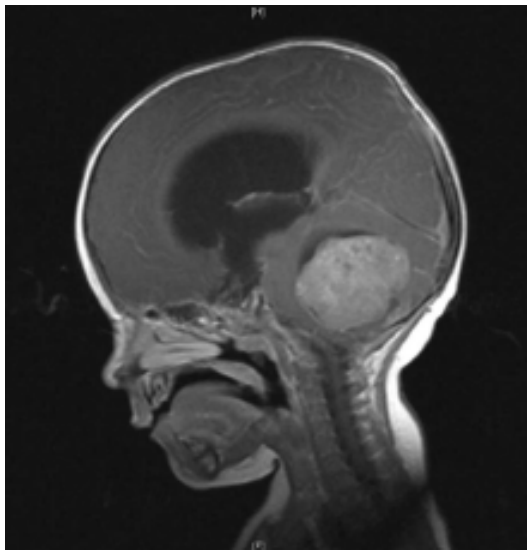

Figure 1. MRI image of head showing medulloblastoma (*Desouza et.al, Frontiers in Oncology, 2014*)

In WNT medulloblastomas, CTNNB1 gene that encodes beta-catenin is highly mutated. Somatic mutations in CTNNB1 cause increased stabilization and localization of beta-

catenin, resulting in deregulation of Wnt signalling pathway[11]. Additionally, it has been identified that many tumors harbouring CTNNB1 mutations have deletions of one copy of chromosome 6[12]. Furthermore, half of Wnt tumors have mutations in DDX3X RNA helicase, which plays role in cell survival and cell cycle[13]. SMARCA4, TP53, KMT2D, and CREBBP are also highly mutated in Wnt medulloblastomas[14]. Since Wnt subtype has a relatively stable genome, patients with Wnt medulloblastoma have better prognosis compared to other medulloblastoma subgroups [15]. Finally, transcriptional profiling revealed that the cellular origin of Wnt medulloblastoma is lower rhombic lip progenitors[16].

SHH is the second common subgroup of medulloblastoma and patients with SHH medulloblastomas have an intermediate prognosis[2]. The unrestrained SHH signalling is the main cause of the development of SHH medulloblastomas. The most common mutation identified in SHH tumors is the mutation of PITCH1. It has been demonstrated that Ptch1 deletions in mice resulted in medulloblastoma[17]. Together with PITCH1 mutations, SHH medulloblastomas harbour mutations in SMO (Smoothened, Frizzled Class Receptor) and SUFU (Suppressor of Fused Homolog) genes. Also, amplification of SHH and transcription factors GLI2 and MYCN have frequently been identified in SHH-subgroups. Whole-genome sequencing of SHH tumors revealed mutations in KMT2D, TP53, BCOR, DDX3X, LDB1, and GABRG1 genes[14,18,19]. Besides, chromosomal losses of 9q, 10q, and 17p have been identified in SHH-subtype medulloblastomas[20,21].

Group 3 medulloblastomas comprise one fourth of all medulloblastoma diagnoses and it is restricted to pediatric patients. Group 3 medulloblastomas have the worst prognosis within four subgroups and many patients do not respond to aggressive therapy[2,4,22]. Amplification of MYC, PVT1, OTX2 and mutations in SMARCA4, CTDNEP, LRP1B, and KMT2D are the most frequent genomic aberrations identified in Group 3 medulloblastomas. Chromosomal structural aberrations such as loss of 10q, 16q, and 17p and gain of 1q and 17q are have also been revealed in Group 3 medulloblastomas[23].

The most common subtype of medulloblastoma is Group 4, comprising about 35% of all medulloblastoma cases and it has an intermediate prognosis[24]. Although Group 4 is the most common medulloblastoma subgroup, the biology of Group 4 subtype is not well-understood. In Group 4 tumors, amplification of MYCN is frequent while Group 3 and WNT medulloblastomas have high expression of MYC proto-oncogene. The most prevalent mutation identified in Group 4 medulloblastomas is the loss-of-function mutation of KDM6A gene, which demethylase histones at H3K27 residues. Moreover, many Group 4 tumors contains mutations in MLL2, MLL3 and ZMYM3 genes[25].

The common features of medulloblastoma subgroups are indicated in **Table 1**.

Table 1. Common features of medulloblastoma subgroups (*Adapted from Northcott, et al. Nat. Rev. Can., 2012*)

	WNT (~10%)	SHH (~30%)	Group 3 (~25%)	Group 4 (~35%)
Overall survival (5 years)	~95%	~75%	~50%	~75%
Cytogenetics Gain Loss	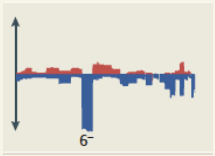	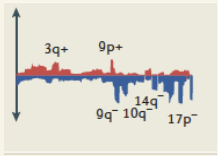	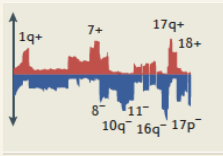	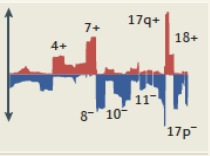
Driver genes	• CTNNB1 (90.6%) • DDX3X (50%) • SMARCA4 (26.3%) • MLL2 (12.5%) • TP53 (12.5%)	• PTCH1 (28%) • TP53 (13.6%) • MLL2 (12.9%) • DDX3X (11.7%) • MYCN (8.2%) • BCOR (8%) • LDB1 (6.9%) • TCF4 (5.5%) • GLI2 (5.2%)	• MYC (16.7%) • PVT1 (11.9%) • SMARCA4 (10.5%) • OTX2 (7.7%) • CTDNEP1 (4.6%) • LRP1B (4.6%) • MLL2 (4%)	• KDM6A (13%) • SNCAIP (10.4%) • MYCN (6.3%) • MLL3 (5.3%) • CDK6 (4.7%) • ZMYM3 (3.7%)
Expression signature	WNT signaling	SHH signalling	• MYC signature • Retinal signature	Neuronal signature

BCOR, BCL6 co-repressor; *CDK6*, cyclin-dependent kinase 6; *CTDNEP1*, CTD nuclear envelope phosphatase 1; *CTNNB1*, β-catenin; EGL; *GLI2*, GLI family zinc finger 2; *KDM6A*, lysine-specific demethylase 6A; *LDB1*, LIM domain binding 1; *LRP1B*, low density lipoprotein receptor-related protein 1B; MLL, mixed lineage leukemia; *OTX2*, orthodenticle homeobox 2; *PTCH1*, patched 1; SHH, sonic hedgehog; *SNCAIP*, α-synuclein interacting protein; *TCF4*, transcription factor 4.

Therapy of Medulloblastoma

1. Radiotherapy

Post-surgical radiotherapy is the standard treatment for patients diagnosed with medulloblastoma. Postoperative craniospinal radiation (CSI; 30-36 Gy) and local boost radiation therapy (RT; 54-56 Gy) is commonly used radiotherapy protocol for children (over 3 years old) with medulloblastoma. The 5-year overall survival (OS) rate for children treated with this protocol is around 46% to 65% in the average-risk group and 50% in the high-risk group[26]. However, intracranial radiotherapy causes profound cognitive disabilities in many patients treated with standard radiotherapy protocols[27].

To minimize the radiotherapy-associated intellectual and neurological disorders, many studies focus on developing new treatment modalities, combining reduced-dose radiotherapy with effective chemotherapy[28].

2. Chemotherapy

Chemotherapy is the fundamental part of medulloblastoma treatment and several different chemotherapeutic agents are used as a standard therapy for medulloblastoma. From those, Vincristine, Cisplatin, Carboplatin, Etoposide, Cyclophosphamide, Lomustine, Methotrexate, and Hydroxyurea are the most common chemotherapeutic agents used in different treatment protocols[29].

Vincristine, the main chemotherapeutic agent used in MB treatment, blocks cell division by interrupting microtubule function. Binding of microtube prevents microtubule congregation and the dividing cancer cells are blocked in mitosis[30,31].

Cisplatin and Carboplatin are platinum-based drugs frequently used in the treatment of cancers, including medulloblastoma. The uptake of the platinum-based drugs result in the formation of Platinum-DNA adducts, activating several cellular responses such as transcription inhibition, cell-cycle and replication arrest, and apoptosis[32].

DNA topoisomerases (Topoisomerase I and II) are the key enzymes for essential cellular processes such as DNA replication, chromosome condensation and segregation. They are essential enzymes for eukaryotic cells and their inhibition results in cell death. Etoposide, one of the most common Topoisomerase II inhibitor, is widely used as a chemotherapeutic agent in MB treatment[33,34].

DNA alkylating agents, such as Cyclophosphamide and Lomustine, destroy highly proliferative cancer cells by incorporating an alkyl groups to DNA and preventing its replication[35,36]. DNA damage induced by alkylating agents results in the apoptosis of cancer cells[37].

Finally, Methotrexate and Hydroxyurea are the antimetabolites to interrupt DNA and RNA growth. Methotrexate inhibits purine and pyrimidine synthesis by targeting key enzymes in the synthesis pathway[38]. On the other hand, hydroxyurea inhibits ribonucleotide reductase, the enzyme required for the conversion of ribonucleotides to deoxyribonucleotides, and cell division is arrested in the S phase of cell cycle[39].

Relevant scientific literature revealing treatment modalities and their outcomes are indicated in **Table 2**.

Table 2. Treatment modalities and their results for patients with medulloblastoma (*Obtained from Packer & Finlay, The Oncologist, 1996* [29] *and Alberta Health Service*)

Disease	Number of patients	Treatment	Results	Investigator
Posterior fossa medulloblastoma	63	Craniospinal + local-boost radiotherapy + vincristine during radiotherapy + cisplatinum, CCNU, vincristine	• Progression-free survival at five years was 85% ± 6%. • Three patients succumbed to a second malignancy, and the overall five-year, event-free survival was 83% ± 6%. • Children who had received reduced-dose radiotherapy had similar outcomes to those who had received conventional-dose therapy. • Patients with metastatic disease at the time of diagnosis had a five-year, progression-free survival rate of 57% ± 15% as compared to 90% ± 6% for those with localized disease at the time of diagnosis.	Packer, 1994 [40]
Medulloblastoma	233	Radiation therapy or radiation therapy + vincristine during irradiation + postradiotherapy of CCNU + vincristine	• Five-year, event-free survival was 60% for children with brain-stem involvement at diagnosis and 50% for patients treated with radiation therapy alone. • Patients with higher T stages did not statistically benefit from the addition of chemotherapy. • For the 30 patients in the study with the most extensive tumors, event-free survival was markedly better in the group receiving chemotherapy (48% versus 0%; p = 0.006). • Overall survival was also significantly prolonged by chemotherapy for patients with more extensive lesions.	Evans, 1990 [41]
Medulloblastoma	286	Radiation therapy or radiation therapy + vincristine during irradiation + postradiation therapy of CCNU + vincristine	• Children with brain-stem involvement at diagnosis had a significantly higher fiveyear, event-free survival than the children who received radiation alone.	Tait, 1990 [42]
Medulloblastoma	364	Preradiation chemotherapy consisting of vincristine, procarbazine, methotrexate or radiation therapy alone	• Five-year event-free survival was 58% ± 2.7% for all patients. • Five-year event-free survival of 56.3% ±6.5% for patients receiving preradiation chemotherapy versus 52.8% ± 6.1% for postradiation chemotherapy only. • Five-year event-free survival of 75% ± 7.2% to 41.7% ± 8.2% for low-risk disease. • Average-risk patients treated with preradiation chemotherapy and reduceddose radiation therapy had poorer rate of survival (41.7% ± 8% than any other subgroup.)	Bailey, 1995 [43]
PNETs of the posterior fossa and other central nervous system sites	304	Craniospinal + local-boost radiotherapy + concomitant vincristine during radiotherapy + prednisone or “eight-drugs-in-oneday” therapy prior to radiotherapy + craniospinal + local-boost radiotherapy + eight post-radiotherapy cycles of “eightdrugs- in-one-day” therapy	• Event-free survival at a median of four years of follow-up was 55%. • Initially, for children with less-extensive disease at the time of diagnosis and now for the group as a whole,there is a statistical difference in survival in those patients who received the control arm of CCNU and vincristine (event-free, five-year survival 60%) as compared to those who received pre- and postradiation “eight-drugsin- one-day” chemotherapy (five-year, event-free survival 51%).	Zelzer, 1995
Medulloblastoma	71	Postoperative radiation therapy alone or craniospinal radiation + chemotherapy (MOPP regimen of nitrogen mustard, vincristine, prednisone and procarbazine)	• Five-year event-free survival of 68% for patients receiving radiation + chemotherapy. • Five-year event-free survival of 57% for patients receiving radiation alone.	Krischer, 1991 [44]

Non-disseminated medulloblastoma	68	Reduced-dose craniospinal radiation + full-dose local-boost radiotherapy + adjuvant CCNU, vincristine, and cisplatinum chemotherapy	• Overall progression-free survival at three years is 80% ± 6%.	Packer, 1995
Disease	**Number of patients**	**Treatment**	**Results**	**Investigator**
Medulloblastoma	46	12 months of "eight-drugs-in-one-day" chemotherapy	• Median time to progression was six months. • Three-year progression-free survival was 22%. • One relapse beyond 21 months from diagnosis.	Geyer, 1994 [45]
Medulloblastoma	19	Intensive induction chemotherapy (cisplatin + high-dose cyclophosphamide + etoposide + vincristine with G-CSF) followed by a single consolidation cycle of myeloablative chemotherapy (thiotepa + etoposide + carboplatin) with stem cell rescue	• 80% completed induction chemotherapy and proceeded to consolidation. • In 13 eligible children, two-year, event-free and overall survivals from diagnosis are 51% and 61%.	Finlay, 1996
Medulloblastoma	28	N=1: thioguanine + procarbazine + dibromodulcitol + CCNU + vincristine N=4: cyclophosphamide + etoposide + cisplatin N=1: methotrexate + nitrogen mustard + vincristine + prednisone + procarbazine	• No significant difference in OS demonstrated between the patients treated with CT vs. no CT	Kunschner, 2001 [46]
Medulloblastoma	30	N=10 high-risk patients: varying combinations of procarbazine + CCNU + vincristine, Irradiation Brain: 40 Gy (1.8–2 Gy fractions/day) Spine: 36 Gy (1.4–1.8 Gy fractions/day) Posterior fossa boost: 54 Gy	• 5-yr OS rate=65% • 8-yr OS rate=51% • 5-yr DFS rate=69% CT vs. 60% no CT (p=NS)	Abacioglu, 2002 [47]
Medulloblastoma	253	N=146: heterogeneous adjuvant CT regimens (8 drugs in 1 day regimen; carboplatin + etoposide), irradiation Brain: 35 Gy, Spine: 35 Gy and Posterior fossa boost: 54 Gy	• 5-yr OS rate=71% CT vs. 73% no CT • 10-yr OS =58% CT vs. 53% no CT (p=NS)	Padovani, 2007
Medulloblastoma	70	lomustine orally (75 mg/m2) + vincristine intravenous (1.5 mg/m2; max. 2 mg) + cisplatin infusion over 6 h after CSI (70 mg/m2), irradiation Craniospinal: 35.2 Gy Posterior fossa boost: 55.2 Gy	• 4-year EFS=68 ± 7% • 4-year OS=89 ± 5% • Peripheral neuropathy (74%) and haematotoxicity (55%) appear to be more common in adults than children • Histological subtype and tumour location identified as risk factors	Friedrich, 2013 [48]
Medulloblastoma	363	Regimen A: Day 0=CCNU (75 mg/m2), Day 0=cisplatin (75 mg/m2) Day 0, 7, 14=VCR (1.5 mg/m2; max. 2 mg) Regimen B: Day 0=cisplatin (75 mg/m2), Day 0, 7, 14=VCR (1.5 mg/m2; max. 2 mg), Day 21, 22=cyclophosphamide (1 mg/m2), Craniospinal: 2,340 cGy, Posterior fossa boost: 3,240 cGy, Total: 5,580 cGy, 180 cGy/day; 5 days/week	• 8-yr EFS=78.2 ± 2.6% • 8-year OS=83.9 ± 2.4%	Rao, 2014 [49]

Drug resistance in cancer

Chemotherapy is one of the main treatment options for cancer. Many different chemotherapeutic agents such as antimetabolites, DNA alkylating agents, topoisomerase I/II inhibitors, platinum compounds and antimicrotubule agents are commonly used in cancer treatment. However, intrinsic or acquired resistance of cancer cells to chemotherapeutics is the major obstacle in effective therapy of cancer. Intrinsic resistance reveals the pre-existence of resistance-mediating factors in tumour cells before receiving chemotherapy. On the other hand, initially drug sensitive cells may develop resistance during drug treatments and this phenomenon is termed as acquired drug resistance[50].

Genomic and proteomic studies revealed that there are many different molecular mechanisms associated with drug resistance. For example, increased drug efflux ability, reduced drug uptake, activation of survival pathways, inactivation of death signalling pathways, mutations of drug targets, changes in drug metabolism, increased DNA repair and epigenetic alterations may contribute the chemoresistance[51]. General features of drug resistance were shown in **Figure 2**.

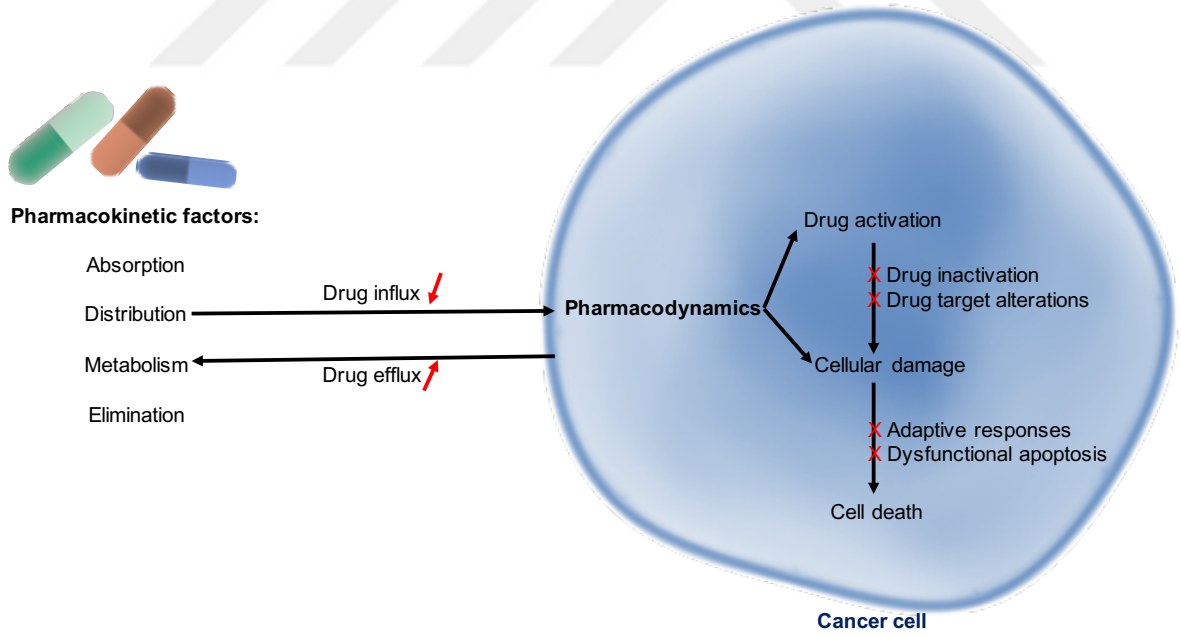

Figure 2.General features of drug resistance in cancer cells. (*Adapted from Holohan et al. Nature Reviews, 2013*)

Additional factors such as elevated prosurvival signals, altered morphology (e.g. EMT), autophagy, DNA damage repair, pathway redundancy, and oncogenic bypass also allow cancer cell to develop resistance[50].

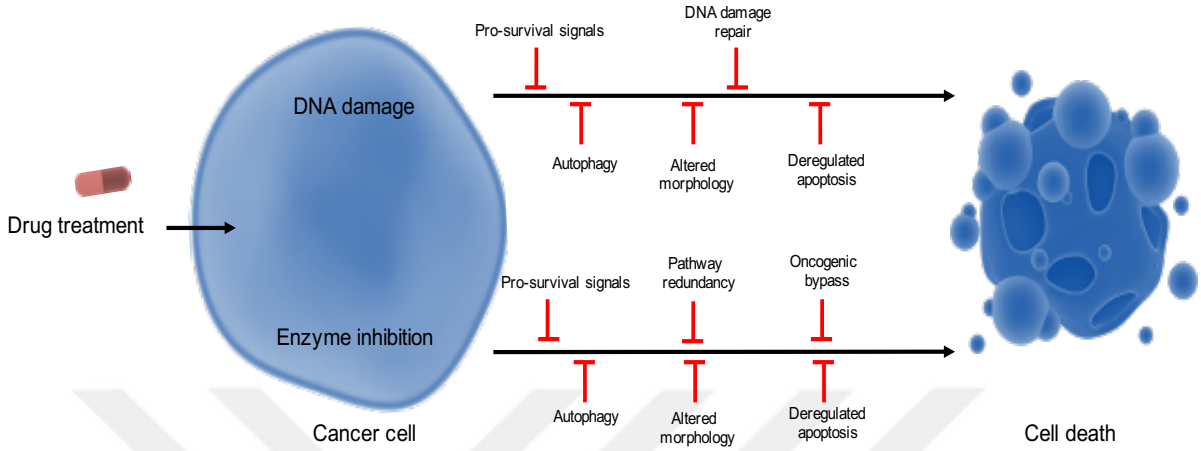

Figure 3. Additional factors contributing drug resistance of cancer cells. (*Adapted from Holohan et al. Nature Reviews, 2013*)

A lot of membrane transporter proteins play role in resistance to commonly used chemotherapeutics by promoting drug efflux. Particularly, transporter proteins from ATP-binding cassette (ABC) transporter family are well studied proteins in multi-drug resistance (MDR). For instance, multi-drug resistance protein 1 (MDR1; P-glycoprotein or ABCB1), MDR-associated protein 1 (MRP1 or ABCC1) and breast cancer resistance protein (BCRP or ABCG2) have substrate specificity ad eliminate various chemotherapeutics, resulting in drug resistance.

As previously described, Vincristine is one of the major microtubule-destabilizing drug used in medulloblastoma treatment. However, cancer cells may develop resistance to vincristine by overexpressing drug-efflux proteins and altering drug targets through mutations. In addition, cancer cells evade vincristine induced cell death by changing the expression of tubulin isotypes, which decreases drug efficacy. Deregulation of apoptotic pathways may also allow cells to develop resistance to vincristine (**Figure 4**).

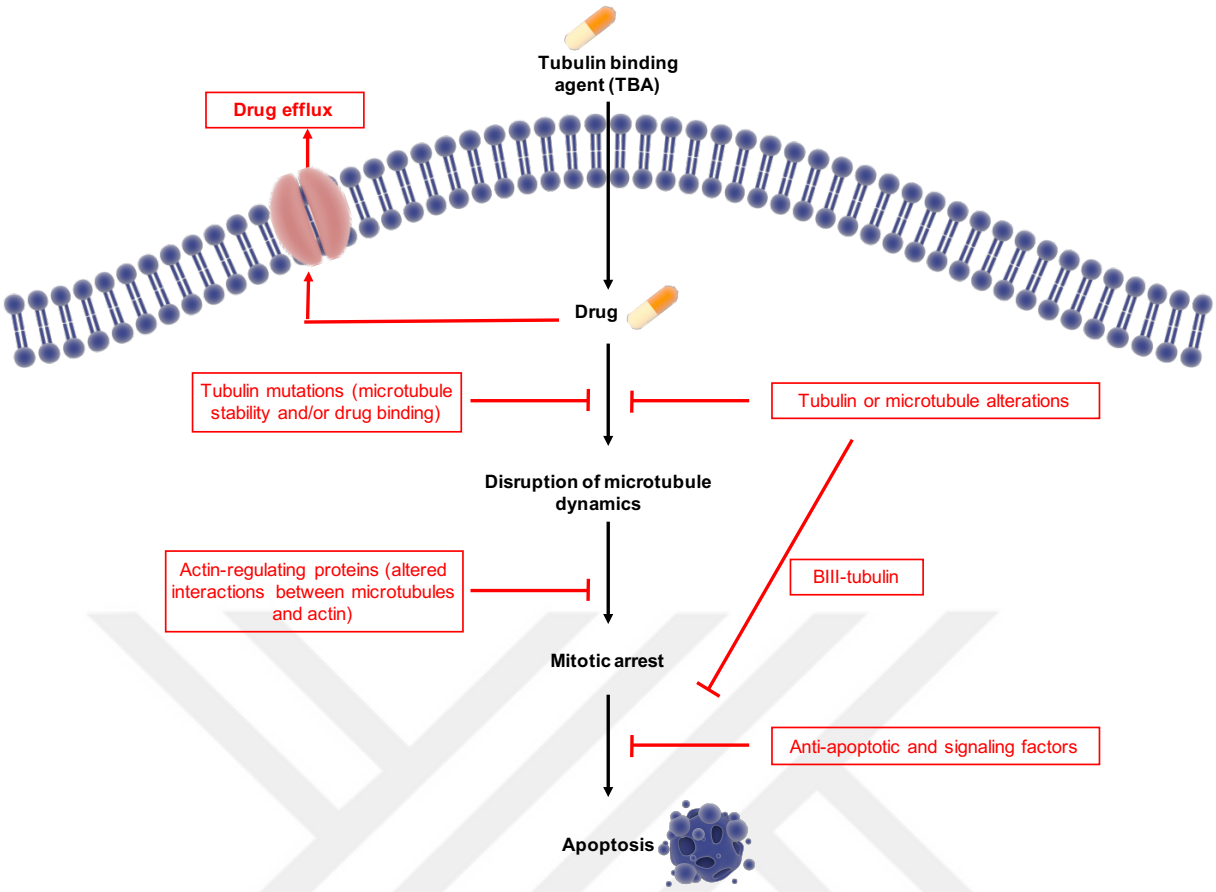

Figure 4. Different mechanisms playing role in resistance to tubulin-binding agents *(Adapted from Kavallaris, Nature Reviews, 2010)*.

Epigenetic deregulation in cancer

Chromatin is a complex of DNA and histone proteins located in the nucleus of eukaryotic cells. The main unit of chromatin is called nucleosome, which contains 147 base pairs of DNA wrapped around positively charged histones (H2A, H2B, H3, and H4). Chromatin has two areas that are termed as heterochromatin and euchromatin. Heterochromatin indicates the tightly packed region of chromatin and mainly it contains inactive genes. On the other hand, euchromatin is the open region of chromatin and it contains actively transcribed genes[52].

Chromatin may undergo many different modifications and these heritable alterations, which are independent of changes in the DNA sequences are defined as “epigenetics”[53]. There are various chromatin modifications and from those DNA and histone methylation, histone acetylation, phosphorylation, ubiquitylation and sumoylation are the most common ones studied in cancer. Chromatin modifications are associated with essential cellular processes such as transcription, replication, repair and condensation/decondensation[54,55].

DNA methylation is the most extensively studied and best characterized epigenetic modification in eukaryotes. DNA methylation mainly occurs on cytosine residue of CpG dinucleotides and generally associated with gene silencing[56,57]. DNA methylation is carried out by DNA methyltransferase (DNMT) enzymes that catalyse the addition of methyl groups from S-adenosyl methionine to DNA[58]. Although five DNMT enzymes have been identified in mammals, namely DNMT1, DNMT2, DNMT3a, DNMT3b and DNMT3L, only DNMT1, DNMT3a and DNMT3b have methyltransferase activity. The members of DNMT enzymes are classified into maintenance and *de novo* DNMTs. The maintenance DNMTs catalyse the addition of methyl groups to hemi-methylated DNA during DNA replication and *de novo* DNMTs (DNMT3a and DNMT3b) are responsible for the methylation of previously unmethylated DNA, respectively [59,60]. Since DNA methylation is one the most important players in gene regulation, its deregulation may result in cancer development. For example, somatic mutations in DNMT3A have been identified in one fourth of patients with acute myeloid leukemia (AML)[61]. Also, DNMT3a inactivation has also been revealed in lymphoma[62].

Besides DNA methylation, epigenetic modifications include the methylation of histone proteins. Histone methyltransferases (HMTs) catalyse the addition of methyl groups to histone on the lysine, arginine and histidine residues. The best characterized histone methylations are H3K4, H3K9, H3K27, H3K36 and H3K79. Whereas H3K4, H3K36, and H3K79 methylations are generally associated with gene activation, H3K9 and H3K27 methylations are correlated with gene suppression[63]. It has been identified that a lot of histone methyltransferases are mutated in many different cancers. For instance, mutations in lysine methyltransferases KMT2A, KMT2B, KMT2C, KMT3A, KMT3B and KMT6 have been identified in several cancers such as medulloblastoma acute myeloid leukemia (AML), acute lymphoid leukemia (ALL), diffuse large B-cell lymphoma (DLBCL), follicular lymphoma (FL) and breast cancer[54].

Another major histone modification is the acetylation/deacetylation of histone on lysine residues. Acetylation of histones is mediated by acetyltransferases and acetylated histone is associated with transcriptionally active open chromatin. Levels of histone acetylation are regulated by opposing activities of the histone lysine acetyltransferases (KATs) and the histone deacetylases (HDACs)[54]. Histone acetyltransferases and deacetylases are crucial enzymes in normal development since they regulate major cellular functions such as cell-cycle regulation, cell proliferation and apoptosis[64]. Therefore, altered expression or mutations in genes encoding HATs and HDACs are have been identified in many cancers. For example, overexpression of HDAC1, a subfamily of HDACs, has been identified in pancreatic, breast, gastric, lung and prostate cancer, resulting in poor prognosis. Moreover, up-regulation of HDAC1, HDAC2 and HDAC3 have been revealed in colorectal, gastric, renal cell and Hodgkin's lymphoma[65]. Mutations in KAT3A (CBP) and KAT3B (p300) histone

acetyltransferases have also been identified in hematological malignancies such as AML, ALL and DLBCL[54].

Histone phosphorylation, another fundamental chromatin modification, is crucial for cellular processes such as DNA repair, replication, transcription, mitosis and apoptosis. The phosphorylation of histones on serine, threonine, and tyrosine residues changes the charge of protein, resulting in conformational change that generally alters the function of protein. Protein kinases mediate the addition of phosphate groups while protein phosphatases remove the phosphate groups from its target protein[66]. Coding mutations, recurrent translocations, and deregulated expression of signalling kinases have frequently been identified in cancers[67].

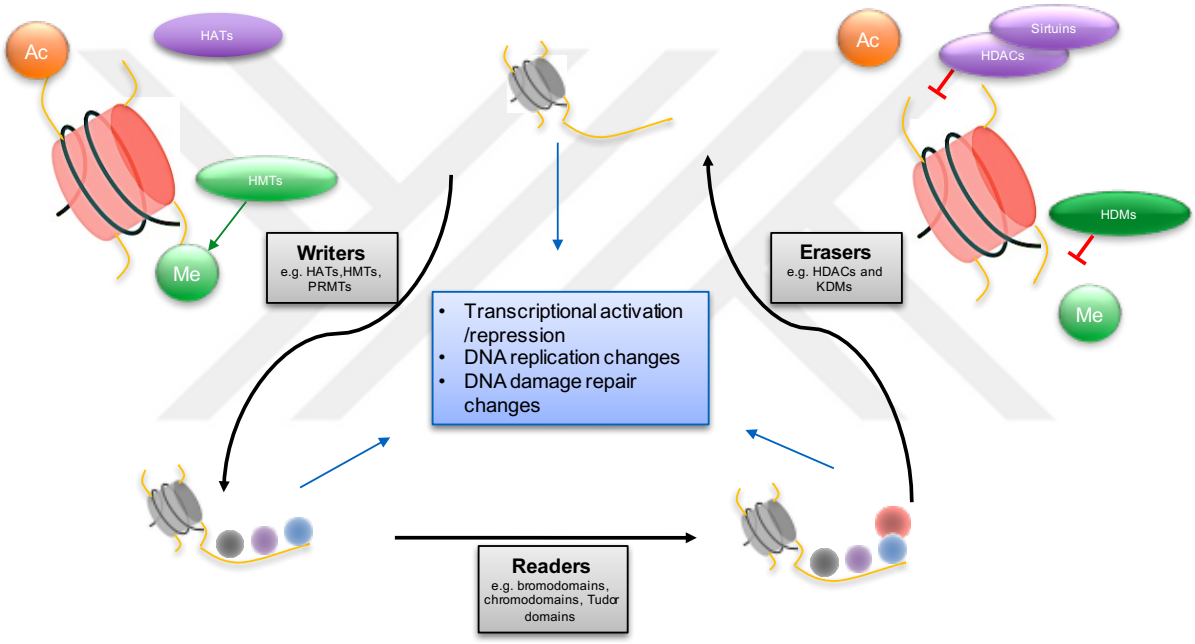

Figure 5. Schematic diagram of chromatin modifying enzymes. (*Adapted from Falkenberg et al., Nat Rev Drug Discov, 2014*)

Medulloblastoma epigenetics

Genomics studies revealed that many histone modifiers, especially histone methyltransferases (HMTs), histone demethylases (HDMs), histone acetyltransferases (HATs) and histone deacetylases (HDACs) are mutated or differentially expressed in different medulloblastoma subgroups, indicating the genomic complexity and heterogeneity of medulloblastoma[14,18,68,69] **(Figure 6).**

Whole-exome and whole-genome sequencing of medulloblastomas identified that KDM6A (UTX), a H3K27 demethylase, is highly mutated in Group 4 medulloblastomas, which have a poor prognosis. Loss-of-function mutations in KDM6A gene result in enriched H3K27me3 phenotype and these H3K27me3 marks maintain undifferentiated state of stem cells by suppressing the expression of lineage-specific genes[68,70,71]. In addition, mutations in KDM6B, another H3K27 demethylase, have also been identified in medulloblastoma[72]. Moreover, it has been showed that overexpression of enhancer of zeste homologue 2 (EZH2) further increases the H3K27me3 enriched phenotype of medulloblastoma cells[73]. EZH2 is an H3K27 methyltransferase and a catalytic subunit of Polycomb repressive complex 2 (PCR2)[74]. Inhibition of EZH2 represses medulloblastoma cell growth and induces apoptosis[75]. Besides, Group 3 and Group 4 medulloblastomas retain their stem-like epigenetic state by inactivating mutations in ZMYM3 (zinc finger, MYM-type 3) and CHD7 (chromodomain helicase DNA binding protein 7) genes, which are H3K4me3 associated chromatin remodellers[14]. Although H3K27me3 enriched phenotype has been identified in Group 3 and Group 4 subtypes (the most aggressive subtypes), how this phenotype contributes the aggressiveness of medulloblastoma is ill-defined. Therefore, uncovering the mechanism of aberrant pattern of H3K27 methylation in detail and targeting specific chromatin modifiers playing role in H3K27me3 enriched phenotype could be a promising therapeutic option in medulloblastoma treatment.

Furthermore, recurrent somatic mutations in H3K4 methyltransferases such as MLL2 (mixed lineage leukaemia 2) and MLL3 have been found in different MB subgroups[72]. Although MLL2 mutations were identified in all subgroups, they were enriched in WNT and SHH subgroups compared to Group 3 and Group 4 medulloblastomas. On the other hand, MLL3 mutations are specific to Group 3 and Group 4 subtypes[68].

SMARCA4 is another chromatin regulator frequently mutated in WNT and Group 3 medulloblastoma. Since SMARCA4 is required for SHH medulloblastoma development and growth, its mutations are rare in SHH medulloblastomas[76].

To add more, KAT6 (lysine acetyltransferase 6A), KDM1A (lysine demethylase 1A), KDM4C, KDM5A, HDAC9 (histone deacetylase 9), BCOR (BCL6 co-repressor), LDB1 (LIM domain binding 1), CREBBP (CREB binding protein), EP300 (E1A-binding protein 300), SETD2 (SET domain containing 2), EHMT1 (euchromatin histone-lysine N-methyltransferase 1), ARID1B (AT-rich interactive domain 1B), REST (RE1-silencing transcription factor), CTCF (CCCTC-binding factor), TLK2 (tousled-like kinase 2) and EYA4 (eyes absent homologue 4) are the chromatin modifiers, which are recurrently mutated in different MB subgroups[68].

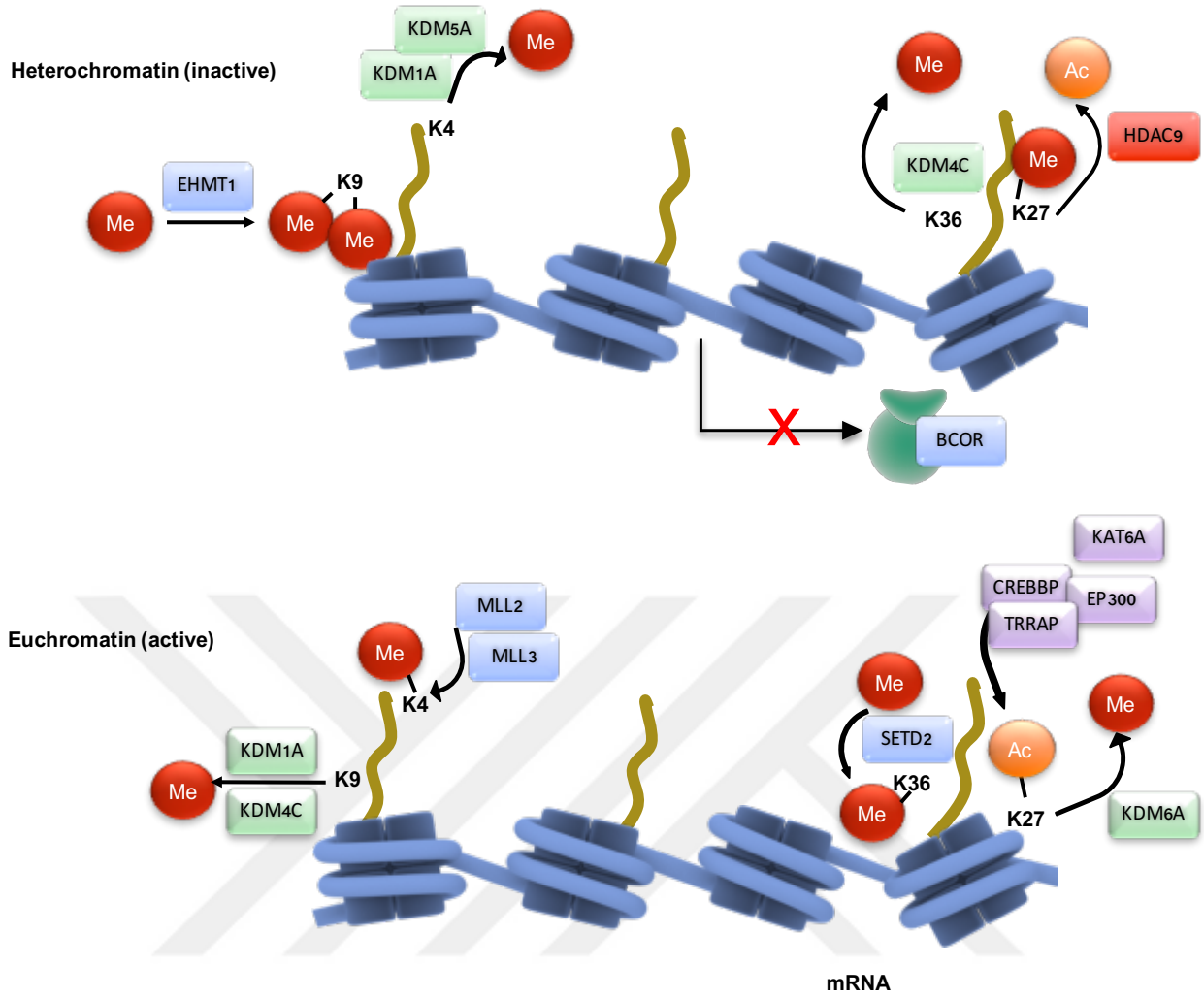

Figure 6. Simplified schematic diagram showing genes that are mutated and/or differentially expressed in medulloblastoma (*Adapted from Northcott et al., Nat Rev Cancer, 2012)*

Chapter 2

Materials and Methods

Cell Culture

Medulloblastoma cell lines DAOY, D283, D341 and human embryonic kidney 293T cell line were purchased from American Tissue Type Culture Collection (USA). Human BJ fibroblasts were kindly provided by Dr. Tamer Onder (Koç University, Turkey). DAOY, D283 and 293T cells were cultured in DMEM (Gibco, USA) supplemented with 10% FBS (Gibco, USA) and 1% Penicillin-Streptomycin (Gibco, USA). D341 cells were cultured in DMEM/F12 medium supplemented with EGF (20 ng/ml), FGF (20 ng/ml), B-27 (Gibco, USA) and 1% Penicillin-Streptomycin (Gibco, USA). All cells were maintained at 37 ^{o}C in a humidified incubator with 5% CO_2.

Chemicals and Reagents

The drug libraries consisting of compounds targeting different chromatin modifying enzymes were provided by Dr. Udo Oppermann (University of Oxford, UK). The list and targets of drugs are indicated in **Table 3** and **Table 4**. GSK-J4, GSK-J5, and IOX-1 were purchased from Cayman Chemicals. In addition, individual drugs namely Belinostat, Vorinostat and 5-Azacytidine were supplied from Prestwick Chemicals.

Chemotherapeutics such as Vincristine (#11764), Cyclophosphamide (#13849), Cisplatin (#13119), Carboplatin (#13112), Methotrexate (#13960) and Etoposide (#12092) were purchased from Cayman Chemicals. Hydroxyurea (#S1896) and Lomustine (#S1840) were supplied from Selleckchem.

Table 3. Epigenetic drug library

Compounds	Class/Target	Working con. (μM)
(+)-JQ1	Bromodomains - BRD2, BRD3, BRD4, BRDT (BET)	0,1
(-)-JQ1 (inactive)	Bromodomains - Negative control	0,1
PFI-1	Bromodomains - BRD2, BRD3, BRD4, BRDT (BET)	5
I-BET	Bromodomains - BRD2/3/4	1
Bromosporine	Bromodomains - pan-Bromodomain	1
CBP/BRD4 (0383)	Bromodomains - CBP, BRD4(1)	5
SGC-CBP30	Bromodomains - CREBBP, EP300	1
I-CBP112	Bromodomains - CREBBP, EP300	1
RVX-208	Bromodomains - BRD2, BRD3, BRD4, BRDT (BET, BD2)	5
SMARCA	Bromodomains - SMARCA, PB1	2,5
PFI-3	Bromodomains - SMARCA2/4, PB1(5)	1
Belinostat	HDAC - hydroxamic acids	5
Valproic acid	HDAC - aliphatic acid compounds	1000
Entinostat	HDAC - ortho-amino anilides	0,5
SAHA	HDAC - hydroxamic acids	1
Trichostatin A	HDAC - hydroxamic acids - Class I & II	0,5
SRT1720	HDAC - SIRT1 (indirect?) activator	1
EX 527	HDAC - SIRT1	1
CI-994	HDAC - 1,2,3,(8)	1
UNC0638	Histone methyltransferase - G9a, GLP	1
UNC0642	Histone methyltransferase - G9a, GLP	1
A-366	Histone methyltransferase - G9a, GLP	2
Chaetocin	Histone methyltransferase - SUV39H1	0,05
PFI-2	Histone methyltransferase - SETD7	2
SGC0946	Histone methyltransferase - DOT1L	7,5
GSK343	Histone methyltransferase - EZH2	3
UNC1999	Histone methyltransferase - EZH2	1
LLY-507	Histone methyltransferase - SMYD2	1
Tranylcypromine	Lysine demethylases - LSD1	20
GSK-LSD1	Lysine demethylases - LSD1	5
GSK J4	Lysine demethylases - JMJD3, UTX, JARID1B	10
GSK J5 (inactive)	Lysine demethylases - Negative control	10
IOX1 (5-carboxy-8HQ)	Lysine demethylases - pan-2-OG	40
Methylstat (Ester)	Histone demethylase	0,5
(E)-JIB-04	Histone demethylase - Pan JmjC	0,05
ML324	Histone demethylase - JMJD2E	5
5-Azacitidine	DNA methyltransferase (DNMT) -	10
5-Azadeoxycitidine	DNA methyltransferase (DNMT) - DNMT1/3	5
Olaparib	Poly ADP ribose polymerase (PARP)	1
Rucaparib	Poly ADP ribose polymerase (PARP)	10
5-Iodotubercidin	Kinase inhibitor - ATP mimetic - Haspin	1
UNC1215	Methyl Lysine Binder - L3MBTL3	5
IOX2	Prolyl-Hydroxylases - PHD2 (EGLN1)	10

Table 4. Epigenetic drug library (updated version)

Compounds	Class/Target	Working con. (μM)
(+)-JQ1	Bromodomains - BRD2, BRD3, BRD4, BRDT (BET)	1
(-)-JQ1 (inactive)	Bromodomains - Negative control	1
PFI-1	Bromodomains - BRD2, BRD3, BRD4, BRDT (BET)	5
I-BET	Bromodomains - BRD2/3/4	1
Bromosporine	Bromodomains - pan-Bromodomain	1
CBP/BRD4 (0383)	Bromodomains - CBP, BRD4(1)	5
SGC-CBP30	Bromodomains - CREBBP, EP300	1
I-CBP112	Bromodomains - CREBBP, EP300	1
RVX-208	Bromodomains - BRD2, BRD3, BRD4, BRDT	5
SMARCA	Bromodomains - SMARCA, PB1	2,5
PFI-3	Bromodomains - SMARCA2/4, PB1(5)	1
PFI-4	Bromodomains - BRPF1B	1
OF-1	Bromodomains - pan-BRPF	5
BAZ2-ICR	Bromodomains - BAZ2A, BAZ2B	1
NI-57	Bromodomains - pan-BRPF	1
LP99	Bromodomains - BRD9, BRD7	1
BI-9564	Bromodomains - BRD9, BRD7	1
NVS-CECR2	Bromodomains - CECR2	1
BAY-299	Bromodomains - BRD1, TAF1	1
I-BRD9	Bromodomains - BRD9	10
Belinostat	HDAC - hydroxamic acids	5
CXD101	HDAC	1
Valproic acid	HDAC - aliphatic acid compounds	1000
Entinostat	HDAC - ortho-amino anilides	0,5
SAHA	HDAC - hydroxamic acids	2,5
Trichostatin A	HDAC - hydroxamic acids - Class I & II	0,5
SRT1720	HDAC - SIRT1 (indirect?) activator	1
EX 527	HDAC - SIRT1	1
CI-994	HDAC - 1,2,3,(8)	1
RGFP966	HDAC - HDAC3	10
PCI-34051	HDAC - HDAC8	5
Rocilinostat	HDAC - HDAC6	10
Tubastatin A HCl	HDAC - HDAC6	10
PCI-24781	HDAC -	10
Romidepsin	HDAC -	1
Mocetinostat	HDAC -	10
Santacruzamate	HDAC 2	50
CPI-360	Histone methyltransferase - EZH2 and EZH1	10
UNC0638	Histone methyltransferase - G9a, GLP	1
UNC0642	Histone methyltransferase - G9a, GLP	1
A-366	Histone methyltransferase - G9a, GLP	2
Chaetocin	Histone methyltransferase - SUV39H1	0,05
PFI-2	Histone methyltransferase - SETD7	2
SGC0946	Histone methyltransferase - DOT1L	7,5

GSK343	Histone methyltransferase - EZH2	3
UNC1999	Histone methyltransferase - EZH2	1
LLY-507	Histone methyltransferase - SMYD2	1
A-196	Histone methyltransferase - SUV420H1/H2	1
BAY-598	Histone methyltransferase - SMYD2	1
Tranylcypromine	Lysine demethylases - LSD1	20
GSK-LSD1	Lysine demethylases - LSD1	0,5
GSK J4	Lysine demethylases - JMJD3, UTX, JARID1B	10
GSK J5 (inactive)	Lysine demethylases - Negative control	10
IOX1	Lysine demethylases - pan-2-OG	40
Methylstat (Ester)	Histone demethylase	2,5
(E)-JIB-04	Histone demethylase - Pan JmjC	0,05
ML324	Histone demethylase - JMJD2E	5
KDOBA67	Histone demethylase	10
KDOAM-25a	Lysine demethylases - JARID	1
KDM5-C70	Histone demethylase - JARID1	10
KDOAM32	Lysine demethylases - JARID	1
KDOPZ32	Lysine demethylases - JARID	1
5-Azacitidine	DNA methyltransferase (DNMT) -	10
5-Azadeoxycitidine	DNA methyltransferase (DNMT) - DNMT1/3	5
Olaparib	Poly ADP ribose polymerase (PARP)	1
Rucaparib	Poly ADP ribose polymerase (PARP)	10
5-Iodotubercidin	Kinase inhibitor - ATP mimetic - Haspin	1
C646	Histone acetyltransferase (HAT) p300/CBP	1
GSK484	Peptidyl arginine deiminase (PAD4)	1
GSK106	Peptidyl arginine deiminase (PAD4)	1
MAZ1805	tRNA synthetase	1
MAZ1392	tRNA synthetase	1
SGC707	Arginine methyltransferase - PRMT3	1
MS049	Arginine methyltransferase - PRMT4, PRMT6	1
MS023	Arginine methyltransferase - Type I PRMTs	1
GSK591	Arginine methyltransferase - PRMT5	1
MS409N	Arginine methyltransferase - PRMT4, PRMT6	1
TP-064	Arginine methyltransferase - PRMT4	1
TP-064N	Arginine methyltransferase - PRMT4	1
CPI-169	Histone methyltransferase - EZH2, EZH1	10
UNC2400	Histone methyltransferase - EZH2	1
A-395	Methyl Lysine Binder - EED	1
A-395N	Methyl Lysine Binder - EED	1
OICR-9429	Methyl Lysine Binder - WDR5	1
UNC1215	Methyl Lysine Binder - L3MBTL3	5
SGI-1776	Kinase inhibitor - Haspin	10
CHR-6494	Kinase inhibitor - Haspin	1
GSK864	Dehydrogenase	5
IOX2	Prolyl-Hydroxylases - PHD2 (EGLN1)	10

Determination of Cell Viability

Cell viability was determined in triplicates via Cell Titer-Glo® (CTG) Luminescent Cell Viability Assay (Promega, USA). CTG determines the number of viable cells by quantifying the ATP, which is an indicator of metabolically active cells. CellTiter-Glo® Reagent lyses cell membrane resulting in ATP release and the amount of ATP is directly proportional to the number of viable cells[77].

CTG assays were performed in the round bottom 96-well plates (Corning®). Cells were seeded into 96-well plates as 2000 cells/well. Next day, cells were treated with the drugs prepared in fresh medium and cultured for 72h. After drug treatment, the media in the wells were discarded and cell were treated with 44 µl of CTG:media mix (1:10). Subsequently, the plates were put into Synergy H1 Reader (Biotek, USA) for 2 minutes of shaking and 8 minutes of incubation at dark. Luminescence read was performed at 560 nm wavelength and the cell viability were revealed as the percentage of viable cells in the treated samples compared to untreated control samples.

Drug screen

Cells were seeded as 2000 cells per well into black bottom 96-well plates. The next day, cells were treated with the drugs targeting different chromatin modifying enzymes. Three days after drug treatment cell viability was measured by CellTiter-Glo assay. In this method, the luminescence readout is directly proportional to number of viable cells (**Figure 7**).

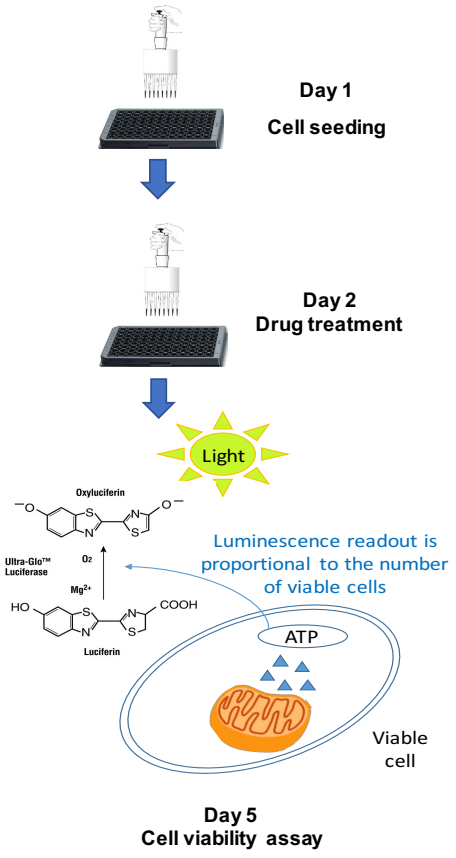

Figure 7. Schematic diagram of the drug screen in DAOY cells. Cells were seeded into 96-well plates and individually treated with drugs in triplicates. CellTiter-Glo cell viability assay was performed after drug treatment for 3 days.

Cloning of shRNA constructs

shRNAs targeting chromatin modifying enzymes were designed using the RNAi Codex and amplified with primer pair indicated below:

Forward: GATGGCTGCTCGAGAAGGTATATTGCTGTTGACAGTGAGCG

Reverse: GTCTAGAGGAATTCCGAGGCAGTAGGC

PCR products were gel-purified and digested with EcoRI and XhoI. Inserts were ligated into the pSMP vector as described. Clones were verified by sequencing and shRNA targeting the firefly luciferase was used as a control. Cloning of shRNAs was conducted by Dr. Tamer Onder (Koç University, Turkey).

Table 5. The sequences of shRNAs used.

shRNAs	**Sequences**
shKDM6A-1	TGCTGTTGACAGTGAGCGACGCGCAAATAGAAATAATTTATAGTGAAGCC ACAGATGTATAAATTATTTCTATTTGCGCGGTGCCTACTGCCTCGGA
shKDM6A-2	TGCTGTTGACAGTGAGCGCCGGAAGGTGCTATTCAAGTATTAGTGAAGCC ACAGATGTAATACTTGAATAGCACCTTCCGATGCCTACTGCCTCGGA
shKDM6A-3	TGCTGTTGACAGTGAGCGCCCACCTACACCTAGTATTTATTAGTGAAGCC ACAGATGTAATAAATACTAGGTGTAGGTGGATGCCTACTGCCTCGGA
shKDM6B-1	TGCTGTTGACAGTGAGCGAGGAGACCTCGTGTGGATTAATTAGTGAAGCC ACAGATGTAATTAATCCACACGAGGTCTCCGTGCCTACTGCCTCGGA
shKDM6B-2	TGCTGTTGACAGTGAGCGCCGCGGCTCGTGTATGTACATATAGTGAAGCC ACAGATGTATATGTACATACACGAGCCGCGTTGCCTACTGCCTCGGA
shKDM6B-3	TGCTGTTGACAGTGAGCGCCCTGTTCGTGACAAGTGAGAATAGTGAAGCC ACAGATGTATTCTCACTTGTCACGAACAGGATGCCTACTGCCTCGGA

Viral Packaging

HEK 293T cells were used for viral packaging as they are easily transfected and allow high expression of viral proteins. In Day 0, 293T cells ($2,5x10^6$ cells/plate) were seeded into 10 cm plates in DMEM supplemented with 10% FBS. Next day, 2500 ng plasmid DNA, 2250 ng GagPol (pUMVC for retroviral, 8.2dVPR for lentiviral packaging) and 250 ng VSVG were mix in serum-free DMEM in a final volume of 200 µl. Subsequently, 20 µl of Fugene HD

Transfection Reagent (Promega, USA) and 180 µl of serum-free DMEM were mixed and incubated at room temperature for 5 min. Afterwards, 200 µl of DNA mixture and 200 µl of Fugene mixture were combined and incubated at room temperature for 30 min. Thereafter, 293T cells were transfected and incubated at 37 ^{o}C overnight. After overnight incubation, the media was refreshed with 8 ml of DMEM supplemented with 10% FBS. Approximately 48h and 72h post-transfection, virus containing media was collected and filtered through 0.45 µm filters (Millipore, USA) by syringe. Viral supernatants were aliquoted and stored at -80 ^{o}C. All virus producing cells, plates, tubes, filters and syringes were incubated with bleach and discarded.

Establishing a puromycin kill curve in DAOY cells

Puromycin kill curve of DAOY cells was established to determine the optimal puromycin concentration required to eliminate non-transduced cells. DAOY cells were treated with different concentrations of puromycin (0,06 µg/ml to 2,50 µg/ml) and the viability of cells was measured by Cell Titer-Glo cell viability assay.

Quantitative real time PCR

Firstly, NucleoSpin RNA isolation kit (Macherey-Nagel, Germany) was used for extraction of RNAs from cells. The amount and purity of isolated RNA were measured by the NanoDrop. cDNAs were synthesized as following: 1000 ng of purified RNA, 2,5 µl of 2 mM dNTPs (Life Technologies, USA), 1 µl of Random Hexamer (Invitrogen, USA) and dH_2O were assembled into an RNase-free tube and incubated at 65 ^{o}C for 5 min. Subsequently, the tubes were transferred on ice and supplemented with 5 µl of 5X First Strand Buffer (Invitrogen, USA), 2 µl of 0.1M DTT (Invitrogen, USA) and 0,5 µl of RNAsin (Promega, USA). The tubes were incubated for 10 minutes at room temperature and 1 µl MMLV-RT enzyme (Invitrogen, USA) was added. The reaction mix was vortexed briefly and incubated at 37 ^{o}C for 1 hour and then 70 ^{o}C for 15 minutes. When the reaction was completed, 75 µl of nuclease free water was added into each reaction tube. Finally, 10 µl of 2X LightCycler® 480 SYBR Green I Master (Roche, Germany), 1 µl of 5 µM primer mix, 7 µl nuclease free water and 2 µl of cDNA were assembled in a 96-well opaque white plate (Roche, Switzerland) and the relative mRNA expression levels were detected by $2^{-\Delta\Delta CT}$ method via LightCycler 480 Instrument II. All primers used in qRT-PCR are shown in **Table 6.**

Table 6. RT-PCR primer sequences

Gene		Sequence
hGAPDH	**F**	5'-AGCCACATCGCTCAGACAC-3'
	R	5'-GCCAATACGACCAAATCC-3'
DR4	**F**	5′-ACCTTCAAGTTTGTCGTCGTC-3′
	R	5′-AACTC TCCCAAAGGGCTATGT-3′
DR5	**F**	5′-AAGACCCTTGTGCTCGTTGT-3′
	R	5′-AGGTGGACACAATCCCTCTG-3
CASP-3	**F**	5'-CATGGAAGCGAATCAATGGACT-3'
	R	5'-CTGTACCAGACCGAGATGTCA-3'
CASP-7	**F**	5'-CGGTCCTCGTTTGTACCGTC-3'
	R	5'-CGCCCATACCTGTCACTTTATCA-3'
CASP-8	**F**	5'-ACACCAGGCAGGGCTCAAAT-3'
	R	5'-GCAGGTTCATGTCATCATCCAGTT-3'
CASP-9	**F**	5'-CTTCGTTTCTGCGAACTAACAGG-3'
	R	5'-GCACCACTGGGGTAAGGTTT-3'
PUMA	**F**	5'-GACCTCAACGCACAGTACGAG-3'
	R	5'-AGGAGTCCCATGATGAGATTGT-3'
NOXA	**F**	5'-ACCAAGCCGGATTTGCGATT -3'
	R	5'-ACTTGCCACTTGTTCCTCGTGG -3'
APAF-1	**F**	5'-AATGGCAGGCTGTGGGAAGT-3'
	R	5'-TCCCCCTGGGAAACAACCTTCT-3'
HRK	**F**	5'- CCTACTGGCCTTGGCTGTG-3'
	R	5'-TACAAGTTCCGCCTGCCG-3'
XIAP	**F**	5'-TGTCCTGGCGCGAAAAG-3'
	R	TGCCAGTGTTGATGCTGAAAC-3'
BCL-2	**F**	5'-CAGGGCGATGTTGTCCACC-3'
	R	5'-GGGGAGGATTGTGGCCTTC-3'
BCL-XL	**F**	5'-GGTCGCATTGTGGCCTTTTTC-3'

	R	5'-TGCTGCATTGTTCCCATAGAG-3'
MCL-1	**F**	5'-TGCTTCGGAAACTGGACATCA-3'
	R	5'-TAGCCACAAAGGCACCAAAAG-3'
KDM6A	**F**	5'-TTCCTCGGAAGGTGCTATTCA-3'
	R	5'-GAGGCTGGTTGCAGGATTCA-3'
KDM6B	**F**	5'-CTACCCCCTTCACATGGCAG-3'
	R	5'-CTCTGACTCGTACAGTTGCCC-3'
ABCB1	**F**	5'-ACTCACTTCAGGAAGCAACCA-3'
	R	5'-CGGATTGACTGAATGCTGATT-3
ABCC1	**F**	5'-CCGCTCTGGGACTGGAATG-3'
	R	5'-ATGTAGCCTCGGTCATGTCG-3'
ABCG2	**F**	5'-CTGAGATCCTGAGCCTTTGG-3'
	R	5'-AAGCCATTGGTGTTTCCTTG-3'
LRP	**F**	5'-TGAGGAGGTTCTGGATTTGG-3'
	R	5'-TGCACTGTTACCAGCCACTC-3'

Histone extraction

To extract the histones, Abcam's histone extraction protocol was modified and followed. Firstly, the cells were harvested and washed with ice-cold PBS. Cell pellets were resuspended in Triton Extraction Buffer (TEB: PBS containing 0.5% Triton X 100 (v/v), 2 mM phenylmethylsulfonyl fluoride (PMSF), 0.02% (w/v) NaN3) and lysed on ice for 10 min. The lysate was centrifuged at 6,500 x g for 10 minutes at 4°C. The supernatant was discarded and pellet containing the nuclei was resuspended in half the volume of TEB. Subsequently, the samples were centrifuged as before and the pellets were resuspended in 0.2 N HCl at a density of $4x10^7$ nuclei per ml. Acid extraction was performed at 4 ^oC overnight. After acid extraction, 1 M NaOH (1/5 volume of the HCl) was added and the samples were centrifuged at 6,500 x g for 10 minutes at 4°C. The supernatant containing the histone proteins was collected and protein concentration was measured by Pierce BCA Protein Assay Kit (Life Technologies, USA). The histone extracts were stored at -20 ^oC.

Western Blotting

Cell pellets were lysed with cell lysis buffer containing 1% Nonidet P40 (NP-40), 150 mM NaCl, 1mM EDTA, 50 mM Tris-HCl (pH 7.8), 1 mM NaF, 0.5 mM PMSF, 1X phosphatase inhibitor cocktail (PhosSTOP, Roche, Switzerland) and 1X protease inhibitor cocktail (cOmplete Protease Inhibitor Cocktail Tablets, Roche, Germany) for 30 minutes on ice by vortexing every 10 min. The lysates were centrifuged at 13.000 rpm for 10 min at 4 ^{o}C and supernatants containing proteins were collected. The protein concentrations were determined by Pierce BCA Protein Assay Kit (Thermo Scientific, USA). 4X loading dye consisting of 900 µl of 4X Laemmli sample buffer (Biorad, USA) and 100 µl of beta-mercaptoethanol (Biorad, USA) was prepared and the protein extracts were boiled in 1X loading dye at 95 °C for 10 min. Boiled proteins were stored at -20°C.

For immunoblotting, 10 µg of whole cell extract proteins and 4 µg of histone extracts were run in PROTEAN® TGX™ Gel (Biorad, USA) using 1X TGS running buffer for about 40 minutes. Electrophoretically separated proteins were then transferred from gel to PVDF membrane by Trans-Blot® Turbo™ RTA Mini PVDF Transfer Kit (#170-4272, Biorad, USA). After protein transfer the proteins were visualised on PVDF membrane by Ponceau S staining. Subsequently, the membranes were blocked in 5% non-fat dry milk (Biorad, USA) in 1xTBS-T (20 mM Tris-HCl, pH 7.8, 150 mM NaCl, 0.1%, v/v Tween-20) blocking buffer with gentle shaking at room temperature for 1h. Primary antibodies were prepared in recommended dilutions (**Table 7**) and the membranes were incubated with primary antibodies at 4 ^{o}C with gentle shaking overnight. After overnight incubation, the primary antibody solutions were removed and the membranes were washed three times for 15 min each in TBST. Afterwards, the membranes were incubated with corresponding secondary antibody prepared in 1:5000 dilutions in 5% milk for 1h at room temperature. After washing the membranes three times for 15 min each in TBST, the proteins were detected by Pierce ECL Western Blotting Substrate (Life Technologies, USA) according to manufacturer's instructions.

Table 7. Antibodies used in Western Blot

Antibody	Catalog No	Brand	Dilution
PARP	9542	Cell Signalling	1:1000
GAPDH	sc-25778	Santa Cruz	1:1000
H3K27me3	07-449	Millipore	1:1000
H3 Total	9715	Cell Signalling	1:1000

Trypan blue exclusion assay

Trypan blue is commonly used dye to test cell membrane integrity and the exclusion of trypan blue indicates membrane integrity of living cells. We performed trypan exclusion assay to understand the effect of KDM6A and KDM6B loss on medulloblastoma cell proliferation. Non-infected control, non-targeting shFF, shKDM6A and shKDM6B infected cells were seeded in 10-cm plates (100.000 cells/plates) in triplicates and cultured for 8 days. The average number of viable cells was determined every 2 days by trypan exclusion assay.

Real-time monitoring of cell proliferation

To understand the effect of KDM6A and KDM6B loss on medulloblastoma cell proliferation, xCELLigence Real-Time Cell Analysis (ACEA Bioscience, USA) was used. First, 96-well electronic microtiter plate (E-Plate) was loaded with 100 µl of corresponding medium and background impedance was measured. Afterwards, cells were seeded (2000 cells/well) in 96-well E-Plate in 100 µl and impedance of each well was recorded every 30 minutes for 5 days.

Flow cytometry

Firstly, KDM6A and KDM6B dual knockdown cells were tagged via a lentiviral vector containing green fluorescent protein (GFP) and the transduction efficiency was verified by flow cytometry (BD Biosciences, USA). A mixture of non-tagged shControl cells and shKDM6A/6B-GFP+ cells were prepared (30.000 cells per each cell type) and initial GFP percentage was determined. Subsequently, non-tagged shControl cells and shKDM6A/6B-GFP+ cells were co-cultured in 6-well plates in triplicate. The percentage of GFP+ cells were detected by flow cytometry every three days for nine days.

Establishing vincristine resistant medulloblastoma cell line

To investigate the role of chromatin modifying enzymes (CMEs) in chemoresistant medulloblastoma cells we generated vincristine, commonly used chemotherapeutic agent in MB treatment, resistant medulloblastoma cell line by dose escalation method. Initially, parental DAOY cells were treated with two different concentration of vincristine (1 nM and 2 nM) for 3 months. Subsequently, vincristine concentrations were gradually escalated up to 10 nM and 8 nM, respectively. Control groups were cultured in drug-free medium continuously. After eight months of drug treatment, vincristine resistant DAOY cells having differential response to vincristine were generated successfully. The IC_{50} of vincristine in newly established resistant

cells and parental cells was calculated and fold resistances were determined. All experiments were performed in duplicate (**Figure 8**).

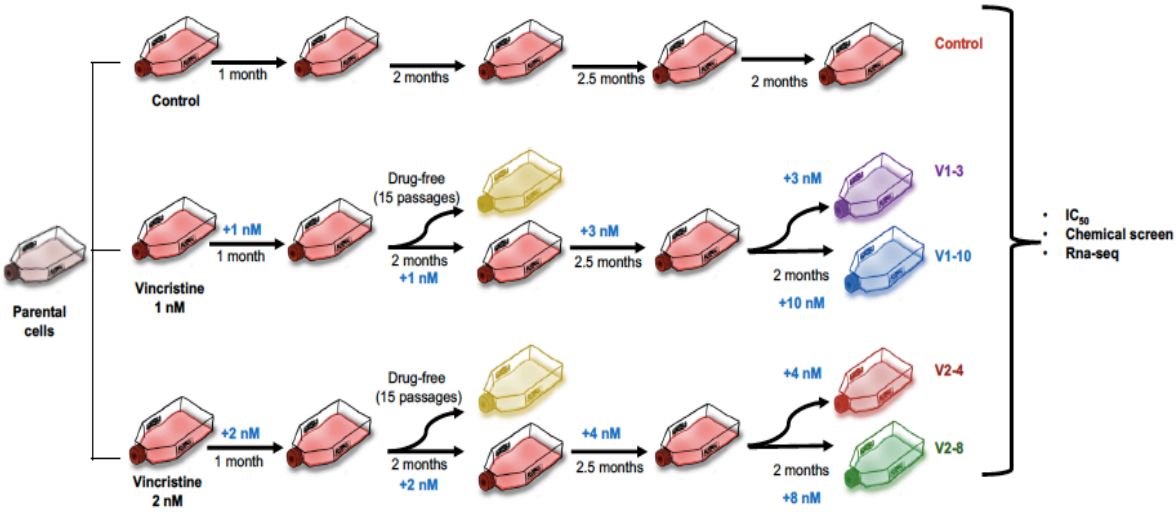

Figure 8. Schematic diagram of establishing vincristine-resistant cell lines by dose-escalation method.

Determining the stability of vincristine resistance

Drug resistant cells might lose their resistance phenotype when they are cultured in drug-free media or when they undergo freeze-thaw cycles. Therefore, we tested the stability of vincristine resistance in newly established resistant cells cultured in drug-free media and in resistant cells underwent freeze-thaw cycles. For this purpose, frozen resistant cells were thawed and cultured in both drug-free and 8 nM vincristine containing media for 10 passages (30 days). The viability of parental and resistant cells was determined by Cell Titer-Glo upon vincristine treatment (4 nM to 64 nM, with 2-fold increases).

Assessing the IC_{50} values of different chemotherapeutics in DAOY cells

Firstly, DAOY cells were seeded into 96-well plates at a density of 2000 cells/well. Next day, the cells were treated with different concentrations of chemotherapeutics and cell viability was determined by Cell Titer-Glo after 72 h drug treatment. The viability of drug treated cells was normalized against that of untreated cells. All drug treatments were applied in triplicate and the IC_{50} values were calculated by using GraphPad Prism 6 software.

Collection of RNA samples for genome-wide transcriptome changes upon KDM6A/KDM6B knockdown and GSK-J4 treatment

To elucidate the functional mechanism of KDM6A/6B in medulloblastoma cells, we will conduct genome-wide profiling of cells upon KDM6A/6B loss. Firstly, we targeted KDM6A and KDM6B by using specific shRNAs and isolated total RNAs of non-transduced control, shControl, shKDM6A, shKDM6B and shKDM6A/6B cells every 3 days for 12 days. Thereafter, differentially expressed genes will be identified by RNA-sequencing (**Figure 9A**).

Secondly, we targeted KDM6A/6B with the H3K27 demethylase inhibitor GSK-J4 to further investigate the transcriptome change upon KDM6A/6B inhibition. For this purpose, DAOY cells were seeded in 6-well plates at a density of 75.000 cells/well. After 24h of cell seeding, cells were treated with DMSO (vehicle control), GSK-J4 (1 μM, 2.5 μM, 5 μM) and GSK-J5 (1 μM, 2.5 μM, 5 μM) in triplicate separately. Pellets were collected after 0, 12, 24 and 48 hours of drug treatment (**Figure 9B**).

RNAs that will be used in RNA-sequencing were isolated by NucleoSpin RNA isolation kit (Macherey-Nagel, Germany) according to manufacturer's instructions.

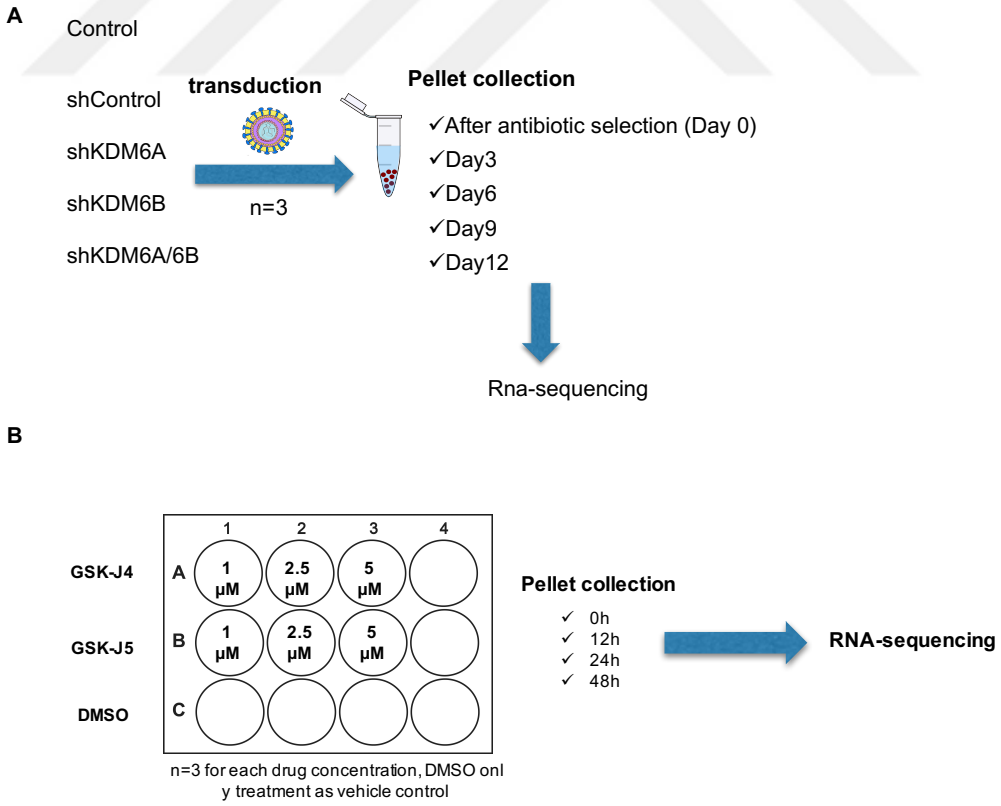

Figure 9. The schematic diagram depicting genome-wide profiling of cells upon KDM6A/6B loss (A) and GSK-J4 treatment (B).

Statistical analysis

We used Student's t-test (two-tailed) to compare two groups. The data were considered significant at $p<0,05$. * denotes $p<0,05$ on the figures.

Chapter 3

Results

Cell density optimization for epigenetic drug screen

CellTiter-Glo cell viability assay was used to determine the optimum cell density and incubation time for DAOY, D341 and D283 cells, which will be used in drug screen. Firstly, DAOY cells were seeded at different numbers (625, 1250, 2500, 5000 and 10000 cells/well) in 96-well plate and the viability of cells was measured every 24 hours for 4 days. According to growth curves, 2000 cells/well was determined as optimum cell density for high-throughput drug screen (**Figure 10**).

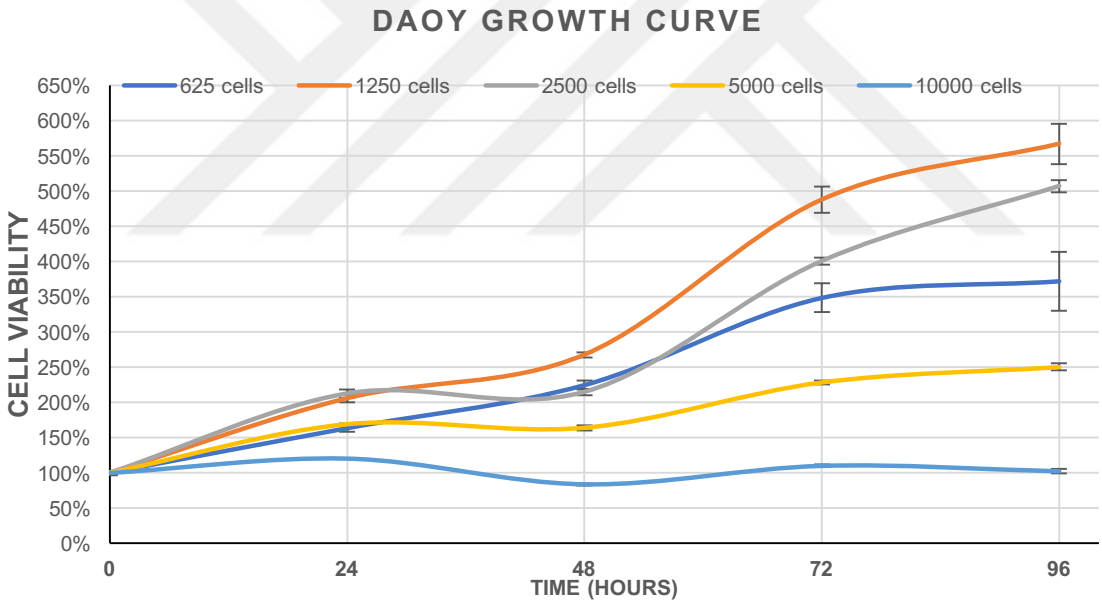

Figure 10. Growth curve of DAOY cells. Cells were seeded at different numbers into 96-well plates and cell viabilities were measured for four days. Cell viabilities were normalized to Day 0 and given as percentages.

In addition, D285 cells were seeded at densities of 5.000, 10.000, 15.000 and 20.000 cells/50 µl/well and cultured for 48 hours. The growth curve revealed that 15.000 cells/50 µl/well was the optimum cell density for the assays that would be conducted in 96-well plates (**Figure 11**).

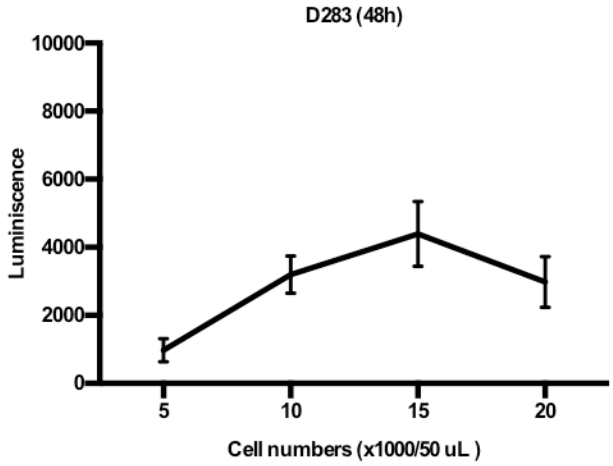

Figure 11. Optimization of D283 cell numbers for viability assays, which will be performed in 96-well plates.

Finally, D341 cells were seeded at different cell densities (20.000, 30.000, 40.000 and 50.000 cells/50 µl) in a final volume of 50 µl and 100 µl growth medium. The viability of cells was measured after 48 hours and 80.000 cells/100 µl/well was determined as optimum cell density for the assays that would be performed in 96-well plates (**Figure 12**).

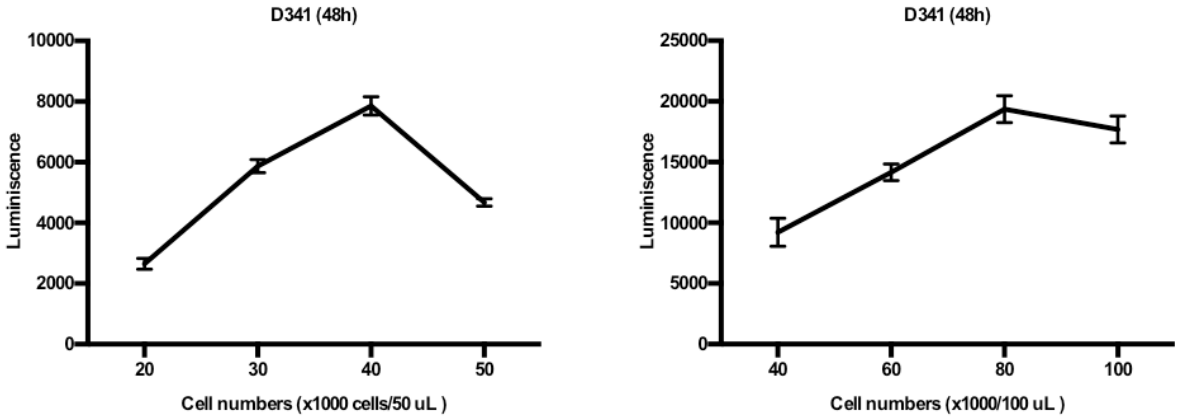

Figure 12. Optimization of D341 cell density for viability assays, which will be performed in 96-well plates.

Epigenetic drug screen in DAOY cells

As previously described, DAOY cells were seeded at a density of 2000 cells/well in 96-well black bottom plates. Cells were treated with the drugs in triplicate after 24 hours of cell seeding and cell viabilities were determined by CellTiter-Glo after 48 and 72 hours of drug treatment (**Figure 13**). The viability of drug treated cells was normalized to untreated control cells and revealed as percent cell viability. The screen hits were defined as compounds that decreased cell viability one standard deviation below mean cell viability. Accordingly, the screen revealed some potential inhibitors that induced cell death in DAOY cells significantly. The screen hits are indicated in **Table 8.**

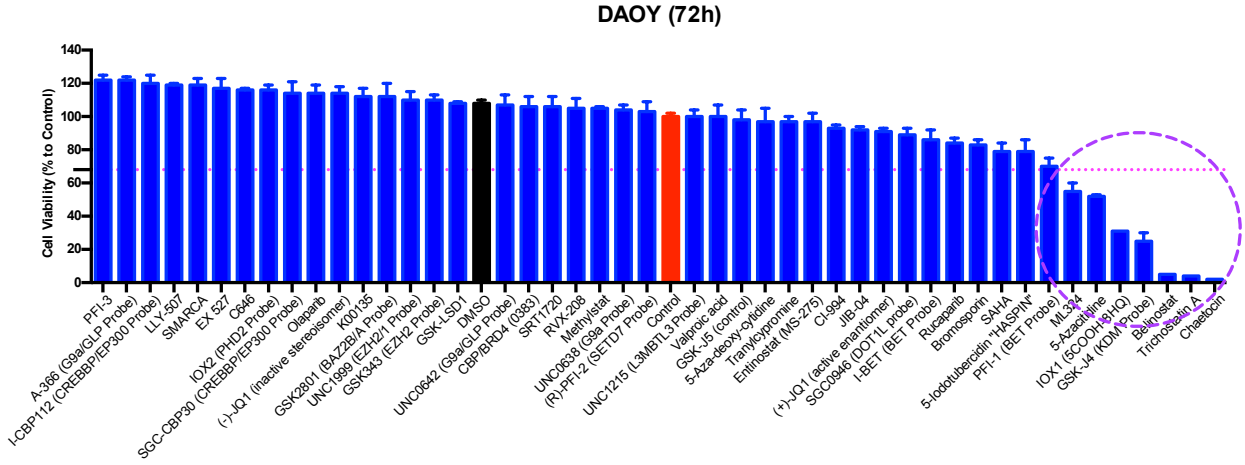

Figure 13. The representative result of two different drug screen performed in DAOY cells. Black bar indicates vehicle control (DMSO) and red bar indicates untreated control cells. Dotted lines denote the significance limit based on one standard deviation (SD) below of average viability. The drugs emerged as screen hits were indicated in purple circle.

Table 8. List of drugs identified as hits from two different drug screens. The viability of drug treated cells was normalized to untreated control cells. Cell viability upon drug treatment was indicated as % viability ± % SEM.

Cell viability (% to Control ± % SEM)					
Targets	**Drugs**	**Screen 1**		**Screen 2**	
		48 h	**72 h**	**48 h**	**72 h**
HDAC	SAHA	68 ± 2	-	-	-
HMT	SGC0946	64 ± 5	55 ± 5	-	-
HDM	ML324	-	55 ± 4	-	55 ± 5
DNMT	5-Azacitidine	53 ± 0,3	39 ± 2	53 ± 4	52 ± 1
HDM	IOX1	-	34 ± 4	63 ± 5	31 ± 0,4
HDM	GSK-J4	49 ± 7	41 ± 12	22 ± 1	25 ± 5
HDAC	Belinostat	17 ± 1	4 ± 0,1	16 ± 0,2	5 ± 0,2
HDAC	Trichostatin A	14 ± 0,3	4 ± 0,1	13 ± 0,3	4 ± 0,3
HMT	Chaetocin	16 ± 1	6 ± 2	7 ± 1	2 ± 0,2

The mechanism of cell death upon drug treatment involves apoptosis

It has been identified that there are many different cell death mechanisms and from those apoptosis, necrosis and autophagy are considered the most common ones[78,79]. To investigate the mechanism of cell death upon drug treatment we focused on apoptosis at first. Some of the well-known apoptotic markers include cleaved caspase-3 (c-cas-3), cleaved laminA (c-lam-A), cleaved cytokeratin-18 (c-CK18), phosphorylated histone H2AX, and cleaved poly(ADP ribose) polymerase (c-PARP)[80].

In this direction, firstly we treated DAOY cells with selected screen hits, namely GSK-J4 (20 μM), IOX-1 (40 μM), Belinostat (5 μM), Vorinostat (5 μM) and 5-Azacytidine (20 μM), and examined the PARP cleavage, which is an indicator of apoptosis, by Western blot. Particularly, IOX-1 and Belinostat treated cells induced PARP cleavage significantly compared to DMSO treated control cells (**Figure 14**).

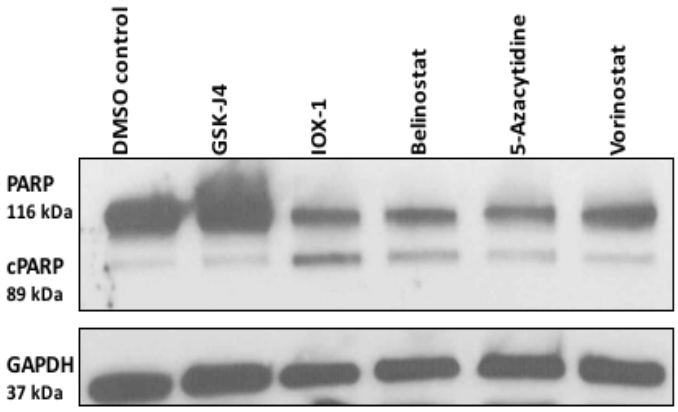

Figure 14. Western blot of PARP cleavage in DAOY cells treated with screen hits. Cells were treated with GSK-J4 (20 μM), IOX-1 (40 μM), Belinostat (5 μM), 5-Azacytidine (20 μM) and Vorinostat (5 μM) for 48 hours.

Since the roles of lysine demethylases (KDMs) are ill defined in medulloblastoma, we focused on GSK-J4 and IOX-1, which are inhibitors of KDMs. To further examine the mechanism of cell death we checked the expression of pro-apoptotic and anti-apoptotic genes upon GSK-J4 (20 μM) and IOX-1 (40 μM) treatment by q-PCR. As shown in Figure 15, GSK-J4 treated cells increased the expression of some pro-apoptotic genes such as Puma, Noxa and Hrk and decreased the expression of anti-apoptotic genes such as Bcl-2 and Bcl-xl, indicating the activation of apoptosis. In addition, IOX-1 treated cells induced the expression of Hrk and decreased the expression of anti-apoptotic genes namely Bcl-2 and Bcl-xl.

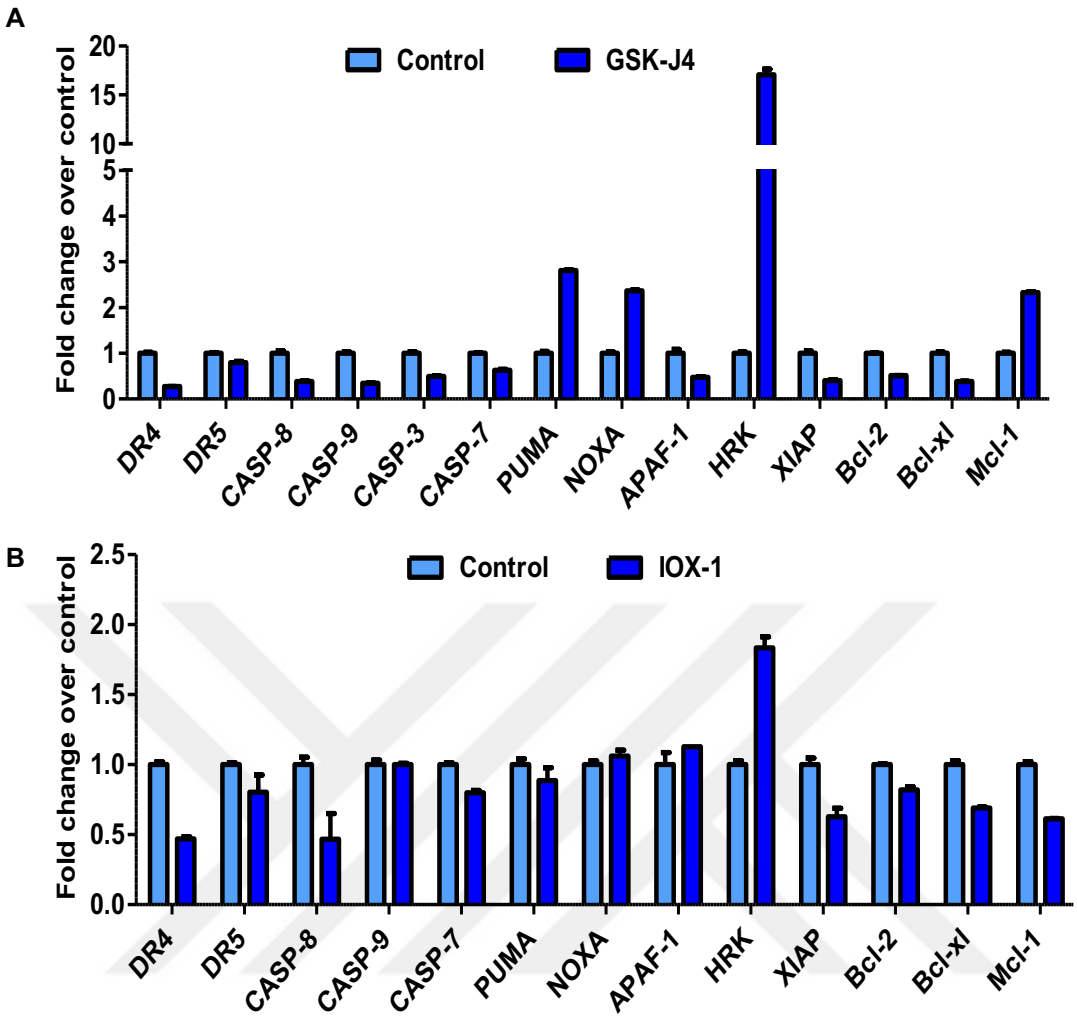

Figure 15. The expression of pro-apoptotic and anti-apoptotic genes in DAOY cells treated with GSK-J4 (**A**) and IOX-1 (**B**) for 8 hours.

Validation of selected hits discovered in drug screen in DAOY cells

In drug screen, the final concentrations of screen hits, namely GSK-J4, IOX-1, Belinostat, Vorinostat and 5-Azacytidine, were 10 μM, 40 μM, 5 μM, 1 μM and 10 μM, respectively. To validate the screen hits and examine whether these hit drugs induce cell death in a dose-dependent manner, DAOY cells were treated with drugs in different concentrations and the viability of cells was measured by CellTiter-Glo assay. In conclusion, these drugs induced cell death in a dose dependent manner in DAOY cells as shown in **Figure 16.**

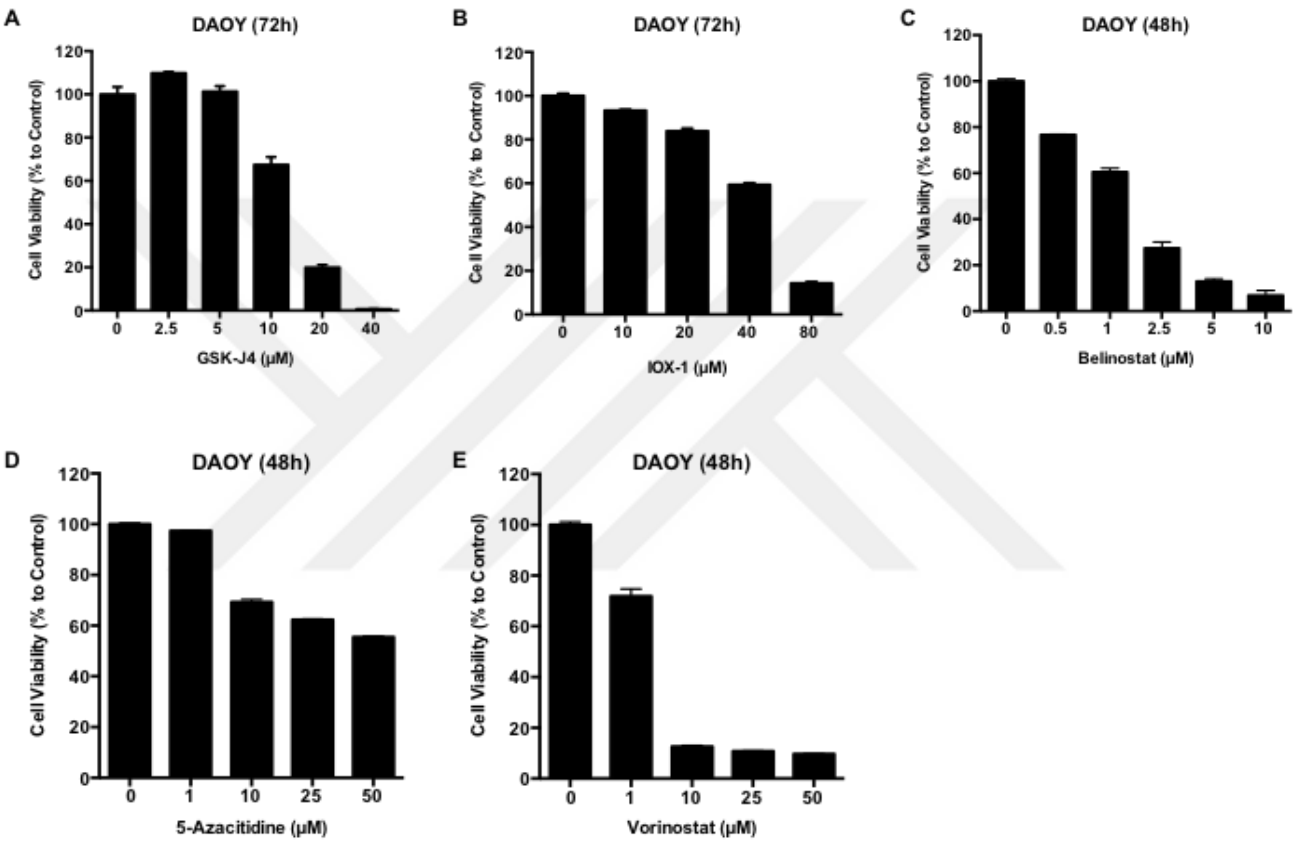

Figure 16. Dose-dependent effects of selected screen hits on DAOY cell viability. Cells were treated with GSK-J4 (**A**), IOX-1 (**B**), Belinostat (**C**), Vorinostat (**D**) and 5-Azacytidine (**E**) in different concentrations and cell viability was measured by CellTiter-Glo.

In addition, we tested GSK-J4 (10 μM) and IOX-1 (40 μM) in D283 cells and we revealed that both drugs reduced cell viability significantly (**Figure 17**).

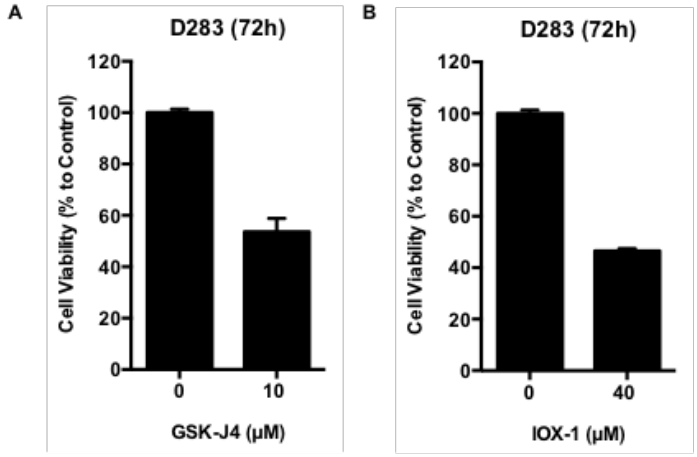

Figure 17. Viability of D283 cells upon GSK-J4 (10 μM) and IOX-1 (40 μM) treatments for 72 hours.

One of the main problems with anticancer drugs is that while many drugs kill cancer cells effectively, they are toxic to non-cancerous normal cells as well. In this direction, we tested screen hits in different concentrations in non-cancerous BJ Fibroblasts to identify potential drugs that were non-toxic to normal cells. As indicated in **Figure 18**, GSK-J4 and IOX-1 were non-toxic to non-cancerous BJ Fibroblasts. In addition, Belinostat, Vorinostat and 5-Azacytidine were relatively non-toxic to normal cells.

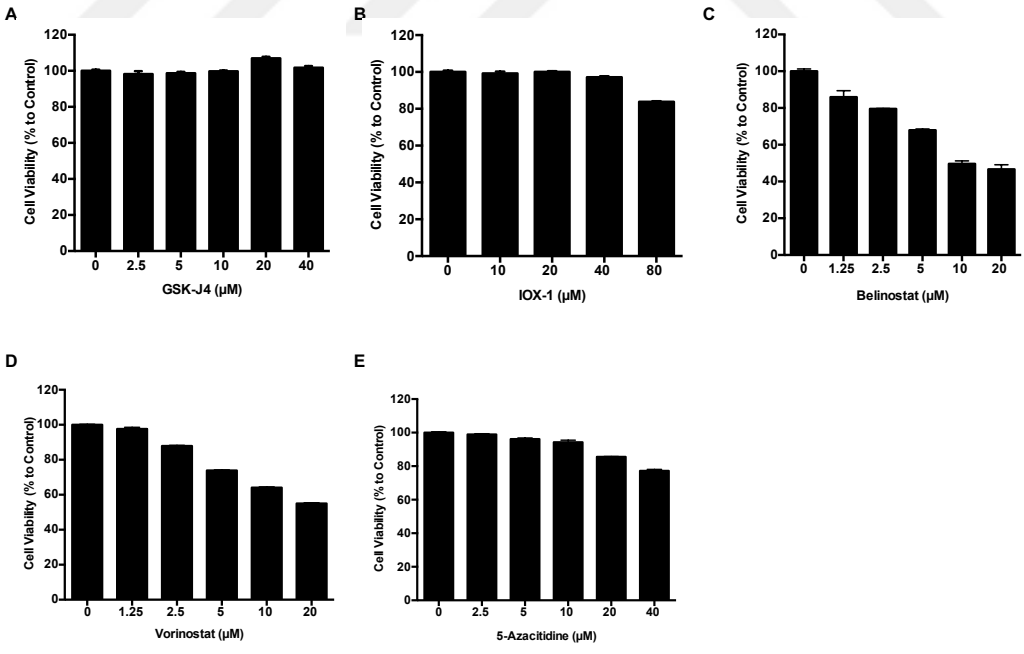

Figure 18. Dose-dependent effects of selected screen hits on BJ Fibroblasts cell viability. Cells were treated with GSK-J4 (**A**), IOX-1 (**B**), Belinostat (**C**), Vorinostat (**D**) and 5-Azacytidine (**E**) in different concentrations and cell viability was measured by CellTiter-Glo.

Puromycin kill curve for DAOY cells

To establish a transduced population of cells it is needed to eliminate non-transduced cells efficiently. Therefore, we developed a puromycin kill curve to determine the optimal puromycin concentration required to kill non-transduced cells. DAOY cells were treated with increasing amount of puromycin and viability of cells was determined by CellTiter-Glo upon 3 days of puromycin treatment. The minimum puromycin concentration required to kill all cells was determined as 1,5 µg/ml as revealed in **Figure 19**.

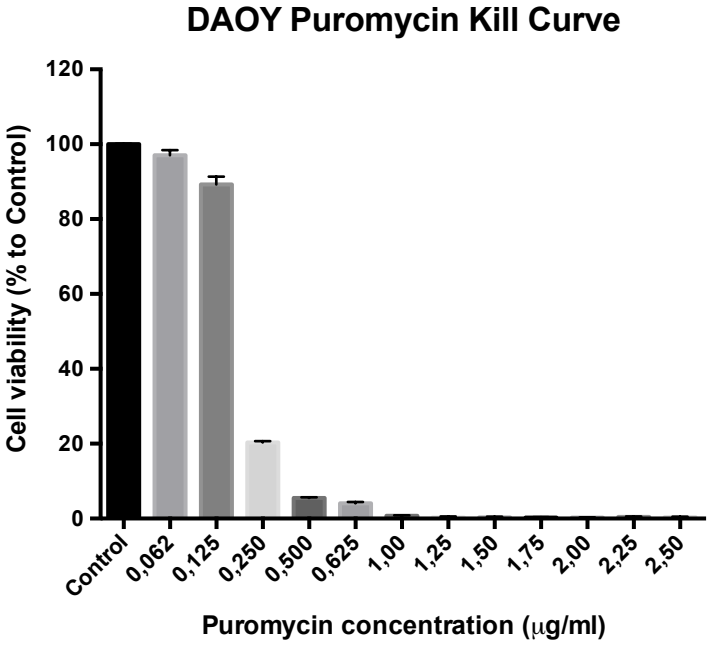

Figure 19. DAOY puromycin kill curve.

Response of DAOY cells to chemotherapeutic agents used in MB treatment

Current therapy of medulloblastoma consists of surgical resection, radiation and chemotherapy. In medulloblastoma treatment many different chemotherapeutic agents are used. For example, Vincristine, Cisplatin, Carboplatin, Cyclophosphamide, Etoposide, Lomustine, Hydroxyurea and Methotrexate are commonly used chemotherapeutics in medulloblastoma treatment[29,81].

Firstly, the response of DAOY cells to commonly used chemotherapeutics was tested by calculating IC_{50} values upon drug treatments. Cells were seeded as 2000 cells/well and treated with chemotherapeutics for 3 days. The viability of cells was determined by CellTiter-Glo and IC_{50} values were calculated by GraphPad Prism software. Whereas DAOY cells showed high resistance to Hydroxyurea and Lomustine (IC_{50} were 716,8 µM and 49,1 µM respectively), they were relatively sensitive to Carboplatin and Cisplatin (IC_{50} were 22,4 µM and 10,2 µM respectively). On the other hand, dose-response curves revealed that DAOY cells were sensitive to Etoposide and Vincristine (IC_{50} were 1,2 µM and 8,6 nM respectively) (**Figure 20**). Accordingly, we established a vincristine resistant medulloblastoma cell line to investigate the mechanism of vincristine resistance and to develop new therapeutic options for therapy resistance in medulloblastoma.

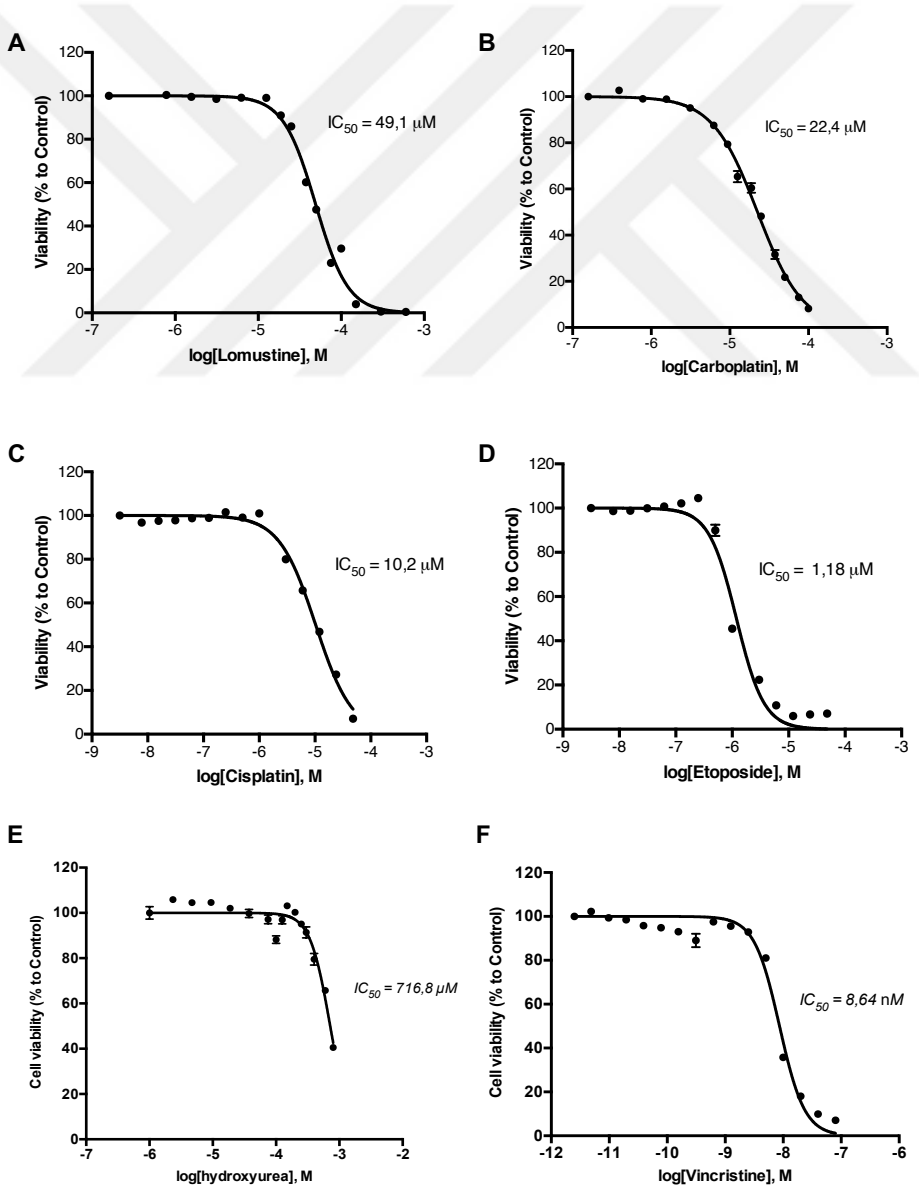

Figure 20. IC50 values of chemotherapeutic agents commonly used in MB treatment. X values indicate doses of drugs on a logarithmic scale and Y values indicate normalized cell viability as percentages. IC50 values were calculated by GraphPad Prism 6.

Vincristine resistant MB cell lines can be generated by dose-escalation method

To investigate the role of chromatin modifying enzymes in chemoresistant medulloblastoma cells, we established a drug-resistant MB cells by dose-escalation method. Since vincristine is one of the main chemotherapeutics used in medulloblastoma treatment, we focused on the function of chromatin modifiers in vincristine-resistant MB cells. For this purpose, DAOY cells were cultured in vincristine-containing medium as previously described and our dose-escalation method generated vincristine-resistant cells, having differential response to vincristine.

Newly established resistant cells were subjected to different concentration of vincristine for 3 days and cell viability was determined by CellTiter-Glo assay. The viability of vincristine-treated cells was normalized to viability of non-treated control cells and dose-response curves were generated by using GraphPad Prism software. IC_{50} values of vincristine for parental and resistant cells were calculated and fold resistances were determined by comparing parental and resistant cells. As shown in **Figure 21**, cells cultured in vincristine-containing media were generated 11 to 89 fold resistance over non-treated parental cells, indicating high resistance to vincristine.

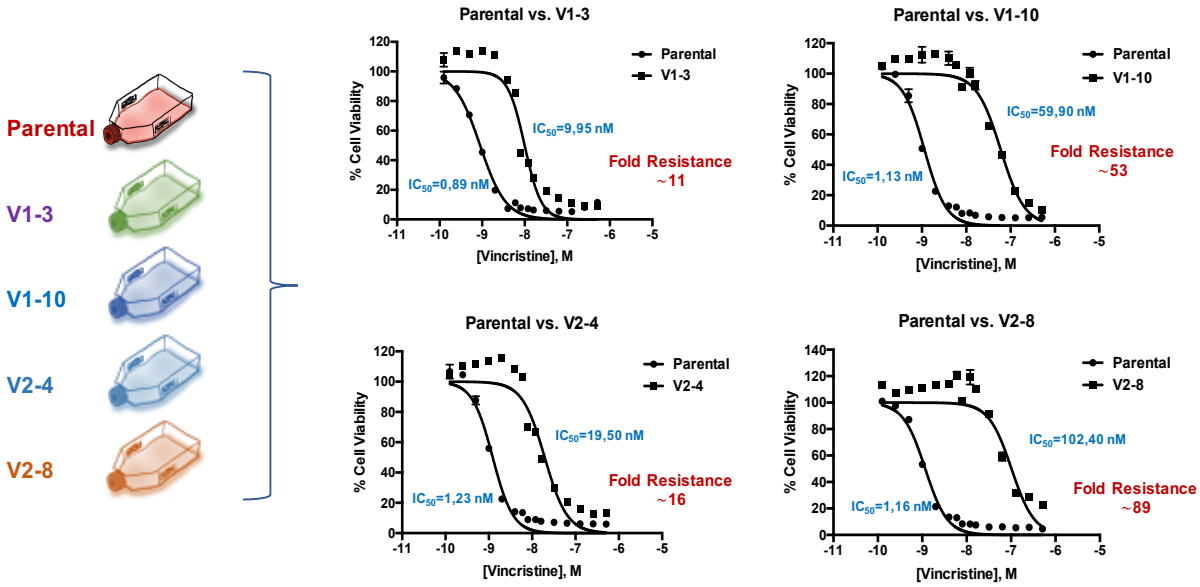

Figure 21. Fold resistance of vincristine-resistant cells compared with its parental cells

Vincristine-resistant cells show increased expression of multidrug resistance genes

To investigate the mechanism of vincristine resistance we examined multidrug resistance (MDR) gene expression of vincristine-resistant cells by quantitative RT-PCR. We determined that vincristine-resistant cells induced the expression of multidrug resistance-associated genes such as ABCC1, ABCG2 and LRP. However, we could not determine the relative expression of ABCB1 gene most likely due to its very low expression in DAOY cells (**Figure 22**).

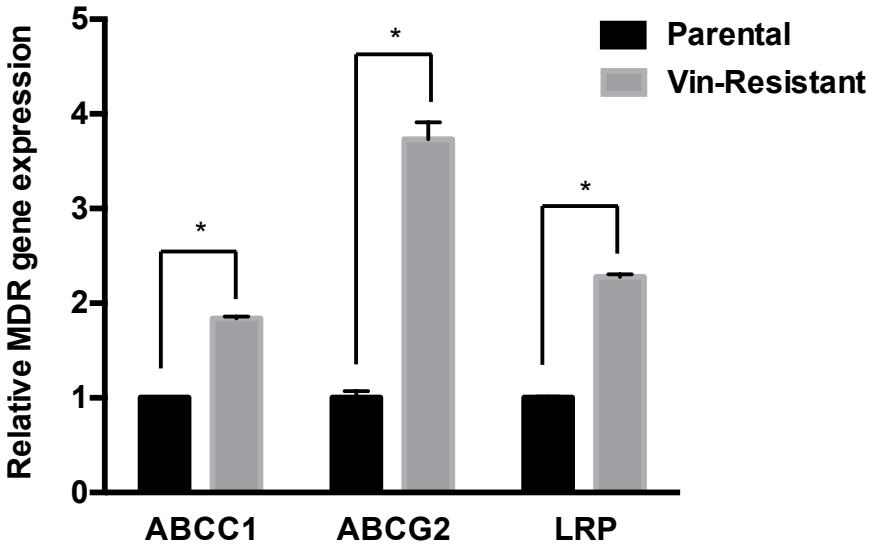

Figure 22. Relative multidrug resistance gene (MDR) expression between parental and vincristine-resistant cells (* denotes p<0,05 t-test).

Vincristine-resistant cells maintain their resistance upon freeze/thaw cycles

Drug resistant cells may lose their drug-resistant phenotype on freeze thaw cycles (reference). Since our project involves examining the role of chromatin modifying enzymes in therapy resistance, we need be sure that newly established vincristine resistant cells maintain their resistance on freeze thaw cycles. In addition, vincristine resistant cells need to preserve their resistant phenotype when they are cultured in drug-free medium. Therefore, we tested the stability of vincristine resistance by measuring cell viability upon vincristine treatments. To this end, a frozen stock of vincristine resistant cells was thawed and cultured in both drug-free and 8 nM vincristine-containing media for 10 passages (about 30 days). Concurrently, untreated parental cells and resistant cells, which did not undergo freeze/thaw cycles were also cultured during stability check. At the end of 30 days, all cells were treated with increasing concentrations of vincristine (4 nM to 64 nM, 2-fold dilutions) for 3 days and viability of cells was determined. **Figure 23** shows the viability of parental and resistant cells upon vincristine treatment.

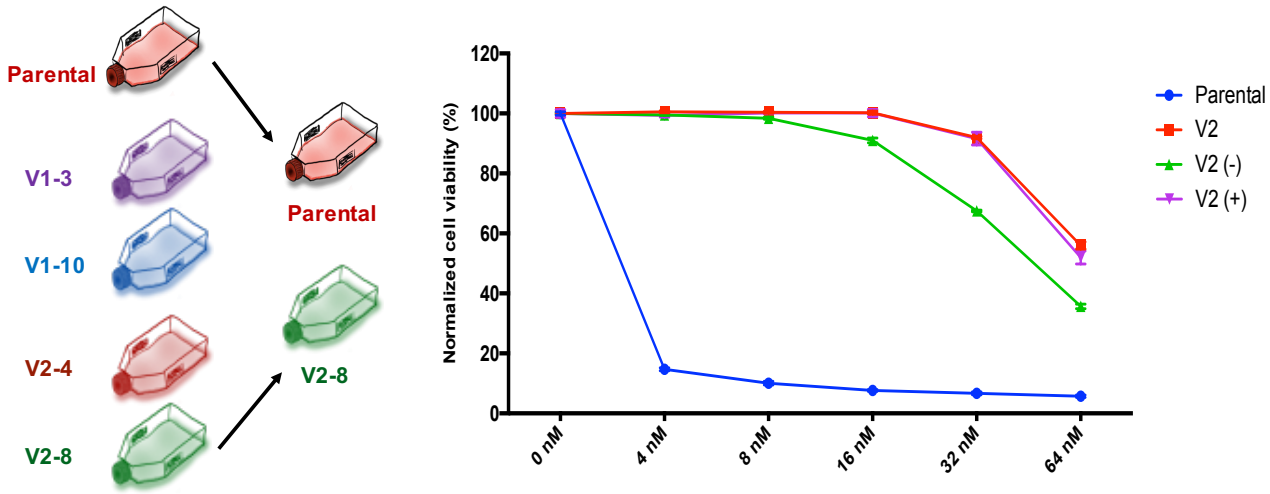

Figure 23. Persistence of vincristine resistance upon freeze/thaw cycles. Parental cells were cultured in drug-free media and V2 cells (as indicated V2-8 on the left) were cultured in vincristine-containing media for 9 months. V2 (-) cells that underwent freeze/thaw cycle were cultured in drug-free media for 10 passages and V2 (+) cells that underwent freeze/thaw cycle were cultured in vincristine-containing media for 10 passages. Cell viability was measured by CellTiter-Glo. Viability of vincristine treated cells was normalized to parental cells.

KDM6A or KDM6B loss do not affect medulloblastoma cell proliferation significantly

To investigate the effect of KDM6A and KDM6B loss on medulloblastoma cell proliferation, three different approaches were used.

Firstly, trypan exclusion assay was performed to examine whether KDM6A and KDM6B loss change the growth rate of medulloblastoma cells. KDM6A and KDM6B were targeted by different shRNAs and shControl was used as non-targeting control. Subsequently, non-transduced control, non-targeting shControl, shKDM6A and shKDM6B transduced cells were seeded in 10 cm plates at a density of 100.000 cells/plates in triplicates and cells were cultured for 8 days. The number of viable cells was determined by trypan exclusion assay and revealed in **Figure 24**.

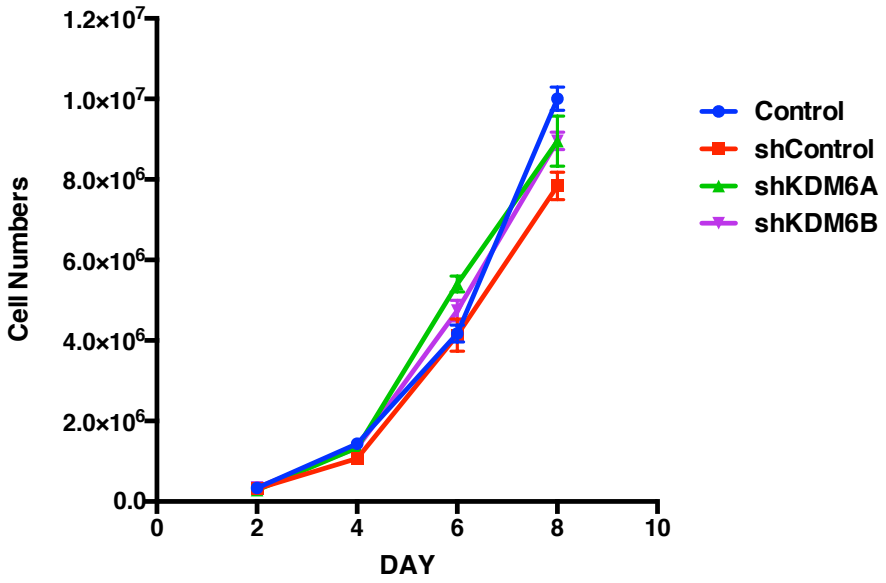

Figure 24. Trypan exclusion assay upon KDM6A and KDM6B loss.

Secondly, we performed xCELLigence Real-Time Cell Analysis to monitor the growth of control, shControl, shKDM6A, shKDM6B and shKDM6A/6B cells for 5 days. As shown in **Figure 25,** loss of KDM6A and/or KDM6B did not affect the growth rate of medulloblastoma cells significantly.

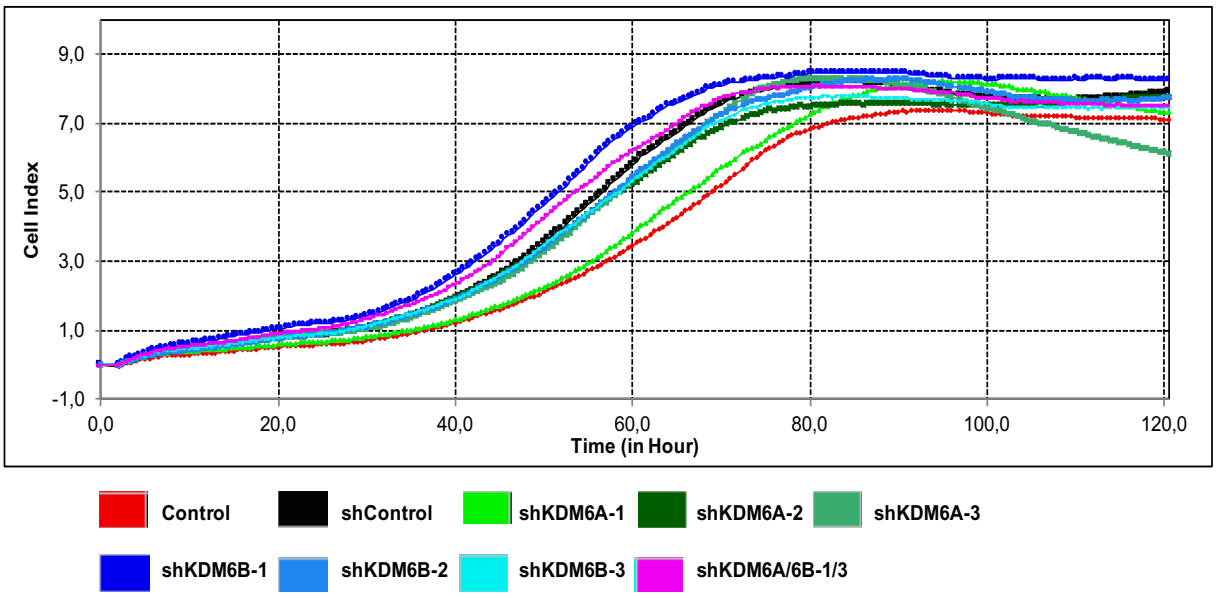

Figure 25. Real-time cell proliferation analysis of control and KDM6A and/or KDM6B knockdown cells

Both trypan exclusion assay and xCELLigence real-time cell analysis revealed that knockdown of KDM6A or KDM6B did not change DAOY cell proliferation. At this point, we speculated that loss of KDM6A or KDM6B might be compensated by the other one as both are H3K27 demethylases. To this respect, we knockdowned both KDM6A and KDM6B expression by shRNAs concurrently (**Figure 26A**) and tagged these dual knockdown cells with GFP. Afterwards, we co-cultured the dual knockdown cells (GFP+) with non-tagged shControl cells in triplicate. Initial GFP percentage was recorded (53% GFP+) and the change in GFP+ cells was detected by flow cytometry every 3 days for 9 days. Three days after cell seeding, the percentage of GFP+ cells shifted from 53,1% to 71,8%. At Day 6, the average percentage of GFP+ cells were 64,4%. The average percentage of GFP+ cells was measured as 53,6% at the end of 9 days (**Figure 26B**).

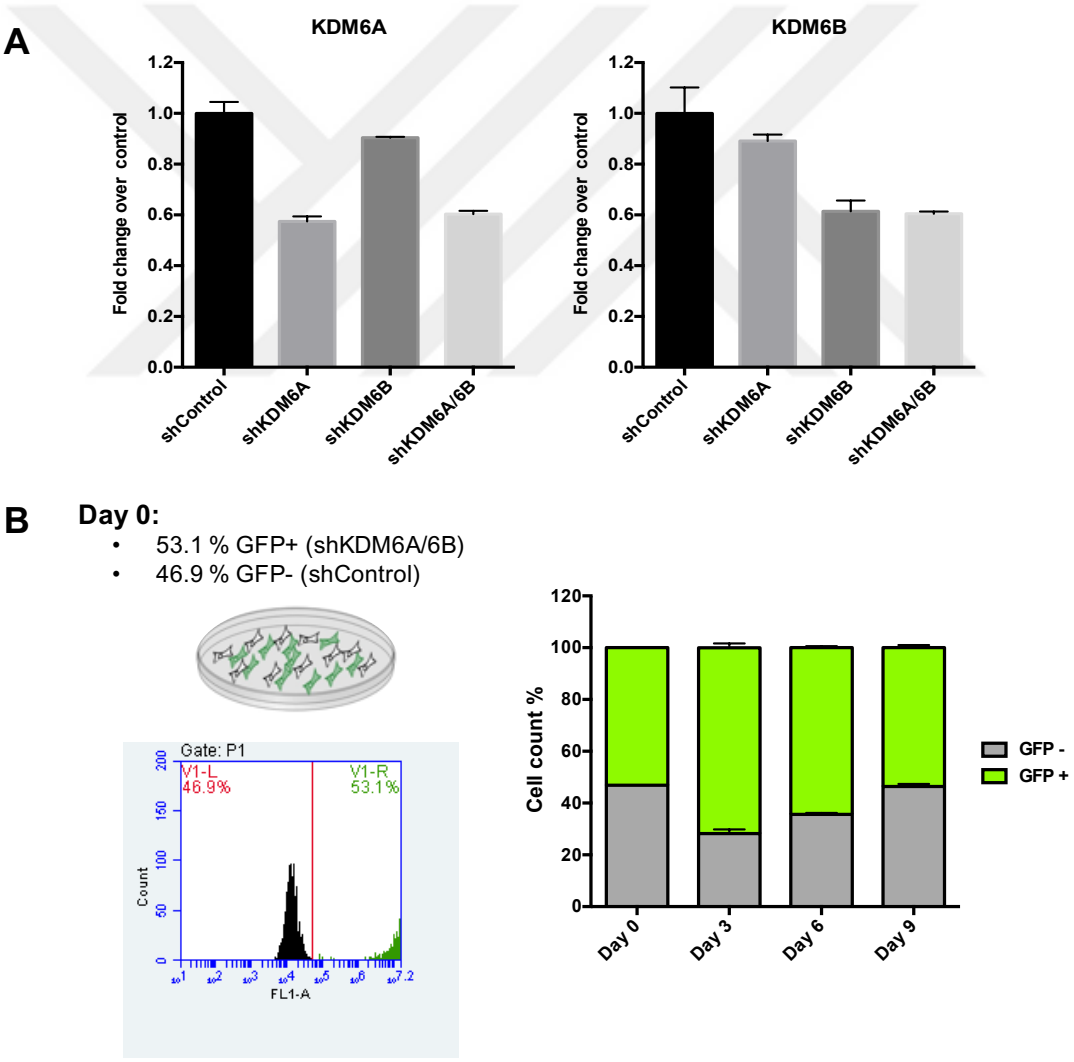

Figure 26. Examining the proliferation rate of DAOY cells upon KDM6A and KDM6B loss. (A) The qRT-PCR result showing KDM6A and KDM6B knockdown. (B) Flow cytometry result of shKDM6A/6B (GFP+) and shControl transduced cells co-cultured for 9 days.

Global methylation changes upon KDM6A/6B knockdown in MB cells

To reveal global methylation change upon KDM6A and/or KDM6B loss, we targeted KDM6A and KDM6B by specific shRNAs (three shRNAs per target). In addition, we generated KDM6A/6B dual knockdown cells by selected shRNAs. We revealed the increase of H3K27me3 mark in shKDM6A-3, shKDM6B-1, shKDM6B-2, shKDM6B-3 and shKDM6A/6B-1/3 cells compared to control cells (**Figure 27**).

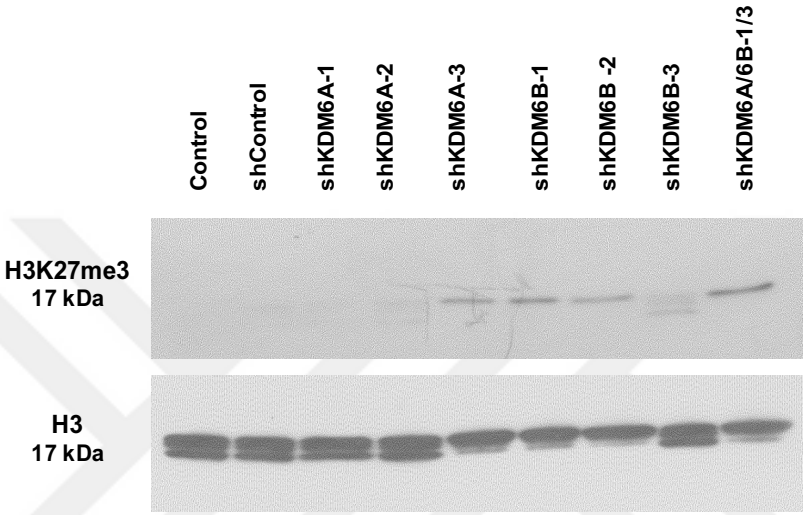

Figure 27. Western blot of global methylation change in H3K27 upon KDM6A and KDM6B loss

The response of cells to vincristine upon KDM6A/6B loss

Since it has been identified that KDM6A and KDM6B are highly mutated in the most aggressive and metastatic MB subgroups (Group 3 and Group 4), we investigated whether there are any effects of KDM6A/6B loss on therapy resistance. Given that vincristine is one of the major chemotherapeutics used in MB treatment, we examined if KDM6A/6B loss affects the response of cells to vincristine.

Firstly, cells were transduced with shRNAs targeting KDM6A and KDM6B as previously described. The efficiency of knockdown was determined by quantitative-real time PCR. Subsequently, non-transduced control cells and KDM6A/6B knockdown cells were treated with different concentrations of vincristine and dose-response curves were obtained as shown in Figure . IC_{50} values of vincristine in control and KDM6A/6B knockdown cells were determined as 2,60 nM and 2,70 nM, respectively (**Figure 28**).

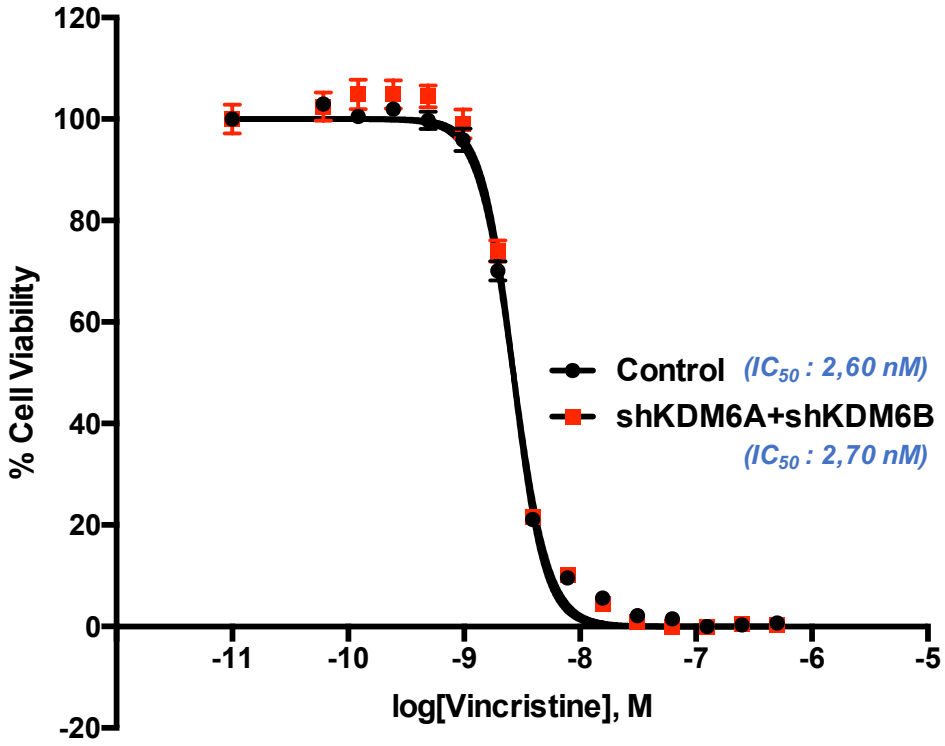

Figure 28. KDM6A and KDM6B loss did not change the response of cells to vincristine. IC50 values were calculated by GraphPad Prism 6 software.

Epigenetic drug screen in parental and vincristine-resistant DAOY cells revealed potential inhibitors that induced cell death

We performed another drug screen by using an updated version of drug library, consisting of 89 inhibitors targeting different CMEs, both in parental and newly established vincristine-resistant cells. The compounds were defined as active if they decreased cell viability one standard deviation below average cell viability. We identified that 8 different HDAC inhibitors (Trichostatin A, Rocilinostat, CXD101, Tubastatin A HCl, Belinostat, Romidepsin, PCI-24781 and Mocetinostat), 2 histone demethylase inhibitors (IOX-1 and KDOBA67), 2 kinase inhibitors (5-Iodotubercidin, SGI-1776), MAZ1805 (Halofuginol) and MAZ1392 (Halofuginone) emerged as hits in our screens performed both in parental (**Figure 29**) and vincristine-resistant cells (**Figure 30**).

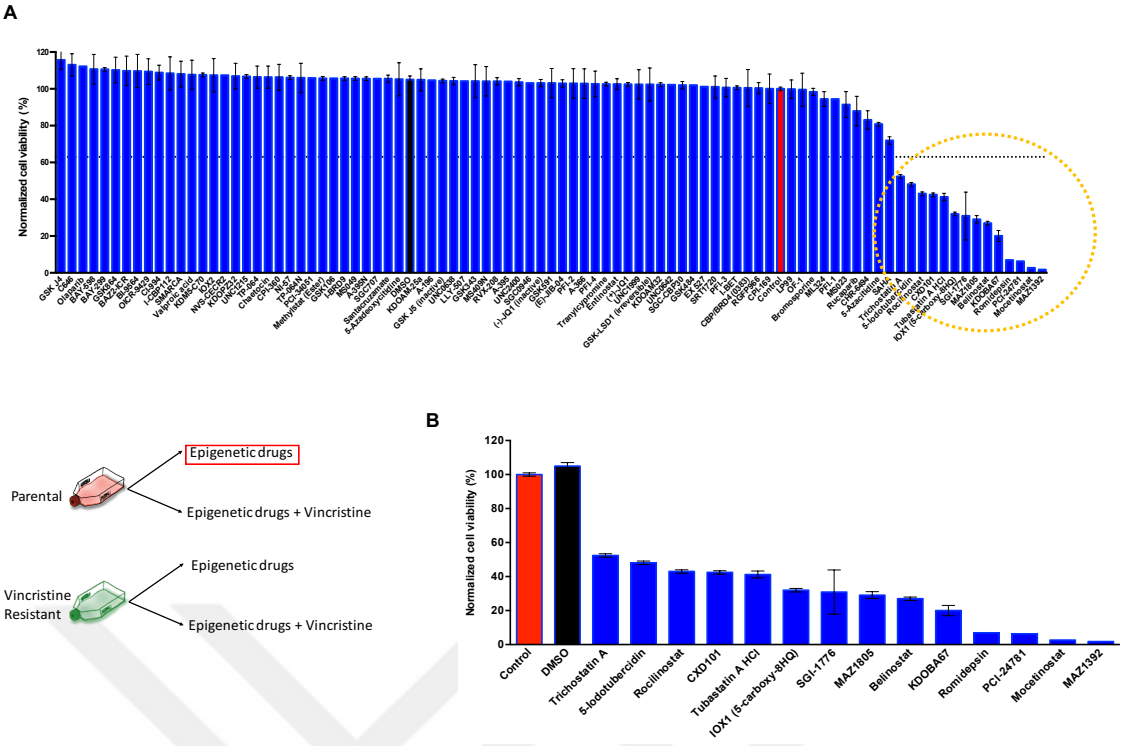

Figure 29. Drug screen in parental DAOY cells with single treatments of epigenetic drugs. (A) Cell viabilities upon drug treatments. (B) Screen hits.

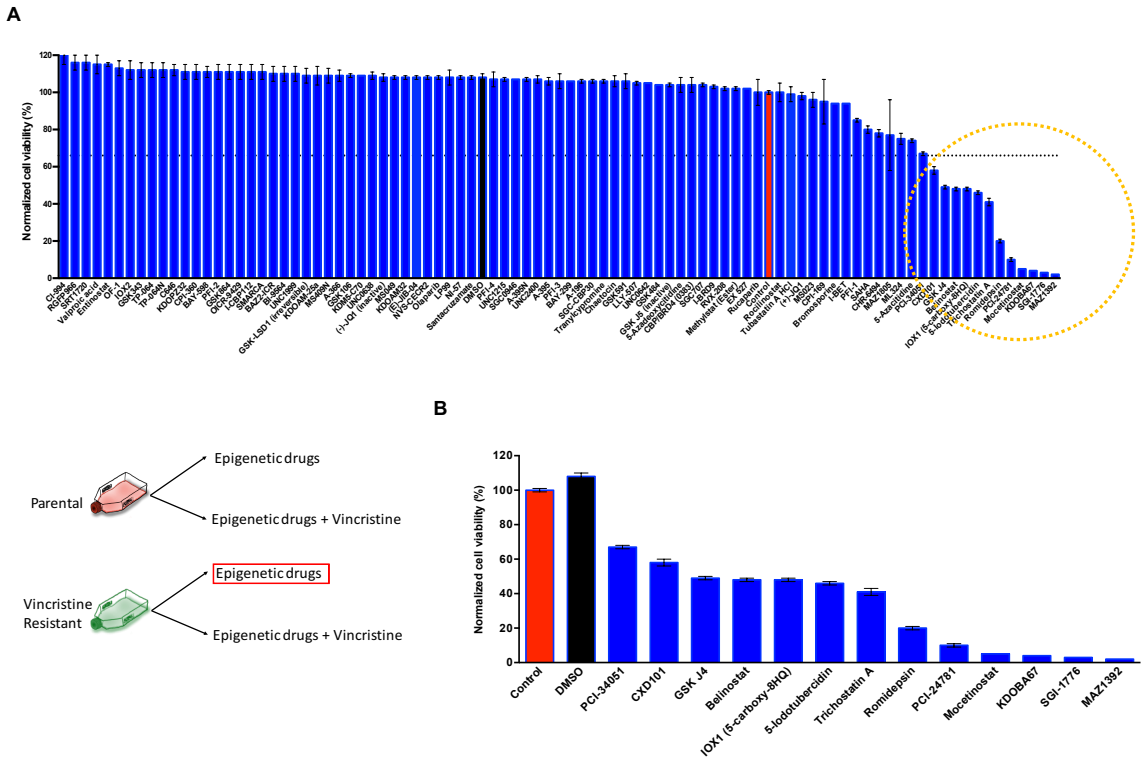

Figure 30. Drug screen in vincristine-resistant DAOY cells with single treatments of epigenetic drugs. (A) Cell viabilities upon drug treatments. (B) Screen hits.

In addition, we tested whether combined treatment of epigenetic drugs and vincristine increased cell death. Firstly, we determined vincristine concentrations that cause 20% growth inhibition in parental and resistant cells as 1 nM and 50 nM, respectively. Accordingly, parental and resistant DAOY cells were treated with epigenetic drugs in combination with vincristine and cell viabilities were measured by CellTiter-Glo.

To this end, parental cells were treated with epigenetic drugs in combination with vincristine (1 nM) for three days and cell viabilities upon drug treatments were revealed in **Figure 31.**

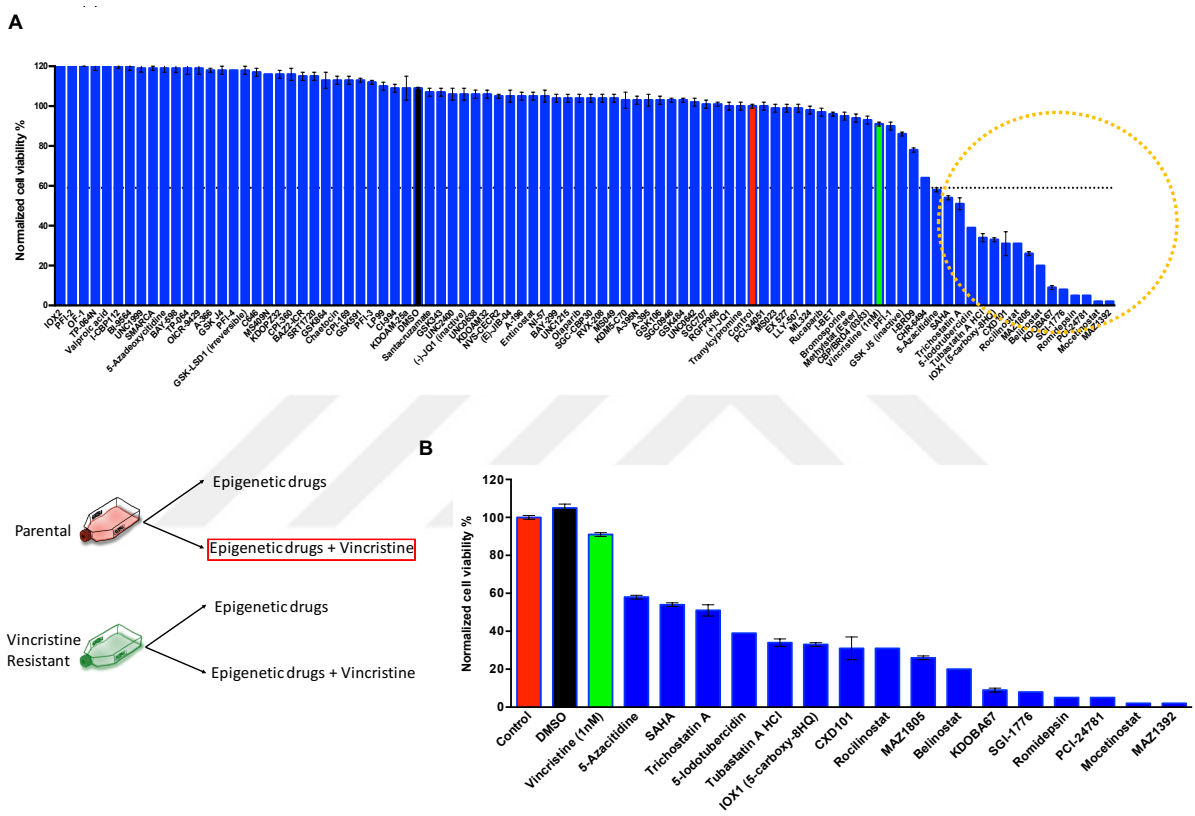

Figure 31. The drug combination screen in parental DAOY cells. (A) Cell viabilities upon combination treatments of epigenetic drugs and vincristine (1 nM). (B) Emerged screen hits.

Furthermore, we performed our drug combination screen in vincristine-resistant DAOY cells to discover novel epigenetic inhibitors that could be used in overcoming vincristine resistance. In this case, resistant cells were treated with epigenetic drugs in combination with vincristine (50 nM) for three days and cell viabilities were indicated in **Figure 32A**. Through this screen, we identified novel drugs that induce cell death in vincristine-resistant cells when they were combined with vincristine (**Figure 32B**).

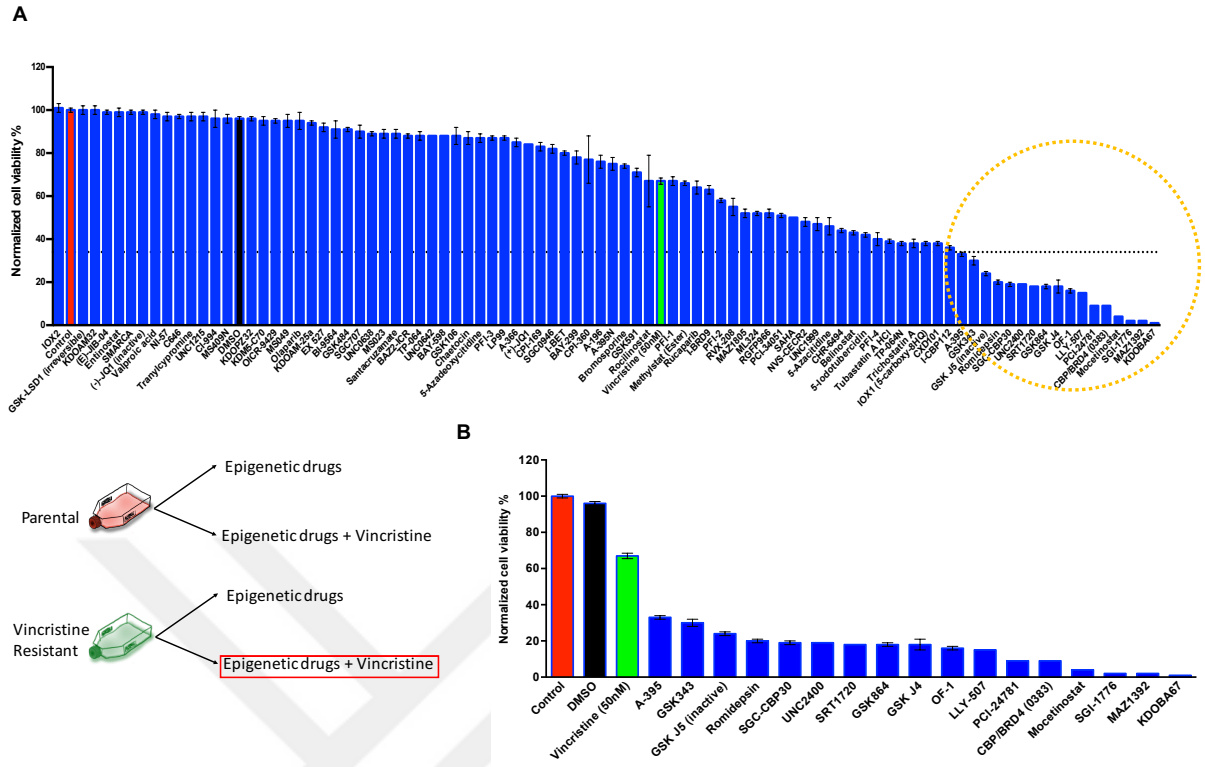

Figure 32. The drug combination screen in vincristine-resistant DAOY cells. (A) Cell viabilities upon combination treatments of epigenetic drugs and vincristine (50 nM). (B) Emerged screen hits.

In conclusion, our drug screen in parental and vincristine-resistant cells revealed that single treatments of Trichostatin A, 5-Iodotubercidin, IOX-1, CXD101, Rocilinostat, MAZ1805, Belinostat, KDOBA67, SGI-1776, Romidepsin, PCI-24781, Mocetinostat and MAZ1392 reduced the viability of both parental and resistant cells significantly. In addition, we have also discovered that combination treatments of A-395, CBP/BRD4, GSK-J5, GSK343, GSK864, LLY-507, OF-1, SGC-CBP30, SRT1720, UNC2400 and Vincristine trigger cell death in resistant cells (**Figure 33**). These results suggest that combination treatments of epigenetic inhibitors and vincristine could be used to overcome vincristine resistance effectively.

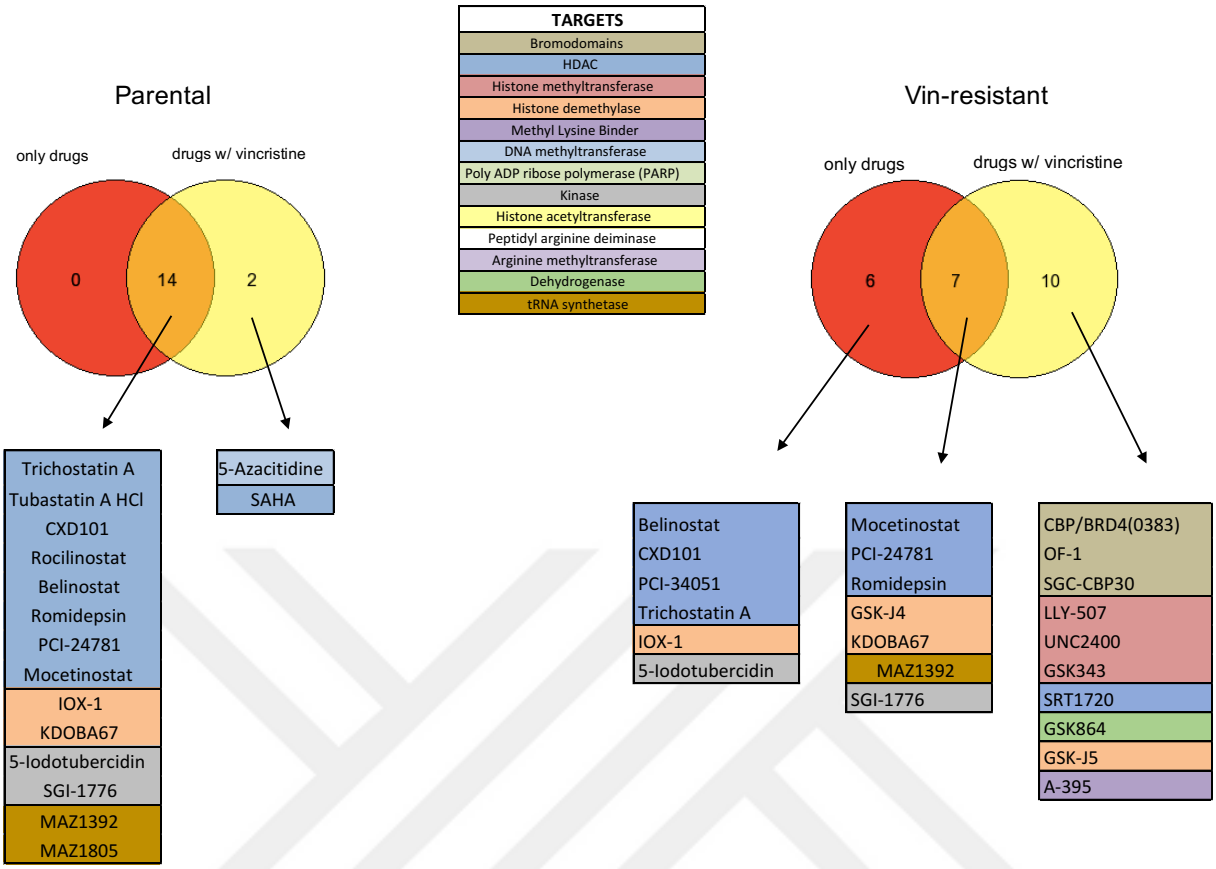

Figure 33. Summary of drug screens performed in parental and vincristine-resistant cells.

Chapter 4

Discussion

Medulloblastoma (MB) is the most common pediatric brain tumor that arises in the cerebellum or medulla/brain stem[18]. It has four different subgroups, which are WNT, SHH (TP53-wildtype or TP53-mutant), Group 3 and Group 4. These subgroups have different transcriptional, cytogenetics, and mutational spectra, making medulloblastoma a complex disease[68,82]. Although standard of care treatment protocols (surgical resection, radiotherapy and chemotherapy) result in high overall survival (OS), many pediatric patients suffer from neurocognitive disorders after treatment[83]. Therefore, novel and more effective treatment modalities are needed.

Genomic studies revealed that various chromatin modifying enzymes (CMEs) are recurrently mutated and/or differentially expressed in medulloblastomas[14,18,68,69]. However, the roles of epigenetic modifiers in the initiation and progression of medulloblastoma are ill-defined. To this end, we mainly focused on epigenetics of medulloblastoma to develop new and more effective therapeutic options.

Firstly, we investigated the role of chromatin modifying enzymes in medulloblastoma by utilizing a chemical library targeting different CMEs. Before performing drug screen in MB cells, we optimized the cell densities and culture conditions of DAOY, D283 and D341 cells at first. According to growth curve of DAOY cells (**Figure 10**), we determined that 2000 cells/well is the optimum cell density for DAOY cells, which will be used in epigenetic drug screens in 96-well plate format. We performed our screens in 96-well plates with three days of drug treatments and determined the cell seeding densities accordingly. Therefore, cell densities should be optimized before starting drug screen if there are any changes in culture conditions and treatment durations. We also optimized the cell seeding densities of D283 and D341 cells for viability assays, which will be performed in 96-well plate format. For D283 cells, the luminescence readout after CTG cell viability assay was significantly higher at a density of 15000 cells/50 µl/well compared to 5000, 10000, and 20000 cells/50 µl/well, revealing the optimal cell density (**Figure 11**). Finally, we determined that optimal cell density for D341 cells, which will be seeded into 96-well plate is 80000 cells/1000 µl/well (**Figure 12**).

In our initial drug screen, we utilized a drug library composing of 46 inhibitors against different CMEs to examine the function of chromatin modifiers in medulloblastoma. We identified some potential inhibitors, such as GSK-J4, IOX-1 and ML324 (HDM inhibitors),

Trichostatin A, Belinostat and SAHA (HDAC inhibitors), Chaetocin and SGC0946 (HMT inhibitors), and 5-Azacytidine (DNMT inhibitor) that induced DAOY cell death significantly (**Table 8**). To validate our screen result, we first determined the dose-dependent effects of selected drugs, namely GSK-4, IOX-1, Belinostat, 5-Azacytidine and SAHA (Vorinostat), on DAOY cell viability. All selected screen hits induced DAOY cell death in a dose-dependent manner.

As the functions of KDMs are ill-defined in medulloblastoma, we mainly focused on GSK-J4, which is a potent inhibitor of KDMs. It has been shown that inhibition of H3K27 demethylase JMJD3 (KDM6B) by GSK-J4 resulted in increased apoptosis, cell cycle arrest and inhibition of clonal growth of pediatric brainstem gliomas harbouring K27M mutation of histone H3.3. Also, HPLC analysis of tissue extracts obtained from brainstem samples revealed detectable GSK-J1 (active product of GSK-J4), indicating permeability of GSK-J4 across blood-brain barrier[84]. However, antitumor activity of GSK-J4 against medulloblastoma cells are not determined clearly. To investigate the effects of GSK-J4 treatment on medulloblastoma cells, we focused on apoptosis at first. Although we determined the upregulation of pro-apoptotic genes such as Puma, Noxa, and HRK upon GSK-J4 treatment, we did not detect the induction of PARP cleavage by Western blot. To further examine whether GSK-J4 induced cell death involves apoptosis, we will perform annexin V staining and TUNEL assay upon GSK-J4 treatment. Since the early stages of apoptosis involves the activation of caspases, we will also check the caspase activities of medulloblastoma cells treated with GSK-J4. The prevention of apoptosis will also be examined upon caspase inhibitor treatment. In contrast to pediatric brainstem gliomas (having reduced H3K27 methylation), loss-of-function mutations of KDM6A/6B and overexpression of Ezh2 methyltransferase result in H3K27me3 enriched phenotype in one of the most aggressive medulloblastoma subgroup (Group 4)[85]. Therefore, it has been considered that hypermethylation of H3K27 contributes to the aggressiveness of medulloblastoma cells. Conversely, we observed that targeting KDM6A and KDM6B (H3K27 demethylases) by GSK-J4 resulted in reduced cell viability in medulloblastoma cells. Since it has been identified that GSK-J4 can also inhibit KDM5 demethylase subfamily[86] (H3K4me3/me2 demethylases), one possible explanation could be that the antitumor activity of GSK-J4 on MB cells involved the inactivation of KDM5 demethylases. GSK-J4 has different inhibitory potential towards KDM6 and KDM5 demethylases at certain concentrations; therefore, the changes in methylation levels of H3K4 and H3K27 should be examined to understand inhibition of which KDM family caused MB cell death upon GSK-J4 treatment. In addition, we will check whether genetic inhibition of KDM6 and KDM5 demethylases by shRNAs could phenocopy GSK-J4 treatment.

In our drug screen in DAOY cells, we also identified HDAC inhibitors namely Trichostatin A, Belinostat and SAHA (Vorinostat) that reduced cell viability significantly. Recent drug screens in medulloblastoma cells have also revealed that HDAC inhibitors such as Panobinostat, Vorinostat and MS-275 potently decreased the growth of MYC-driven medulloblastoma cells[87,88]. DAOY cells more likely represent SHH subgroup of medulloblastoma and our results suggest that targeting histone deacetylases by specific HDAC inhibitors may be a promising therapeutic option for the treatment of SHH medulloblastomas as well.

Starting with GSK-J4, we will also perform apoptotic assays (i.e. TUNEL assay, annexin V staining, caspase activity), cell cycle analysis, colony formation assay, loss-of function experiments with other screen hits, namely IOX-1, ML324, Trichostatin A, Belinostat, SAHA, Chaetocin, SGC0946 and 5-Azacytidine, to investigate the mechanism of cell growth inhibition upon drug treatment.

Although many anti-cancer drugs are efficient to kill cancer cells, they are also toxic to non-cancerous normal cells, resulting in different short and long-term side effects. Therefore, we tested whether these drugs are killing cancer cells and sparing non-cancerous normal cells. For this purpose, we determined the dose-dependent effects of selected screen hits (GSK-J4, IOX-1, Belinostat, Vorinostat, 5-Azacytidine) on BJ Fibroblasts. As shown in **Figure 18**, these drugs were relatively non-toxic to normal cells. To further examine their specificity, we will test these drugs on astrocytes, neural stem cells, and cerebellar granule neurons, which are main populations of cells located in the cerebellum[88].

Despite most of medulloblastoma tumors respond to chemotherapy well, there are still many medulloblastoma patients who do not respond to standard of care chemotherapy. To overcome therapy resistance in medulloblastoma, the mechanisms of drug resistance and molecular players involved in resistance process should be identified clearly. Given that many chromatin modifiers have been identified as mutated and/or differentially expressed in most aggressive and metastatic subgroups (Group 3 and Group 4), we speculate whether chromatin modifiers play role in resistance of medulloblastoma cells to chemotherapeutic agents.

To investigate the roles of chromatin modifying enzymes in chemoresistant MB cells, we had to establish a drug-resistant cell line at first. In the development of drug-resistant cancer lines two main models (clinically relevant model and high-level laboratory model) are commonly used. Clinically relevant models aim to mimic the cycles of chemotherapy treatment in the clinic. In this method, a pulse treatment is used and the doses of drug is low. After drug treatment, the cells are maintained in drug-free media to recover. Compared to high-level laboratory methods, clinically relevant models mimic the cycles of chemotherapy better;

however, they generally result in unstable or low-level resistance and small molecular changes to analyze. On the other hand, cells are continuously cultured in drug-containing media and the doses of drugs are increased over time in high-level laboratory models. High-level models generally generate stably resistant cells and maintaining these newly established resistant cells in culture is easier. Since the level of resistance is higher and the molecular changes are larger in high-level laboratory models, the mechanism of drug resistance can be investigated much more easily[89]. In this direction, we decided to establish a drug-resistant MB cell line by dose-escalation method to elucidate the role of chromatin modifying enzymes in therapy resistance. Firstly, we checked the response of DAOY cells to commonly used chemotherapeutic agents and identified that they were sensitive to vincristine and etoposide, making these drugs suitable for being used in the generation of resistant cell lines (**Figure 20**). Since vincristine is the major drug used in different treatment protocols[29], we decided to establish a vincristine-resistant MB cell line (**Figure 21**). Fortunately, we successfully generated vincristine-resistant cell lines having differential response to vincristine and revealed the stability of resistance upon freeze/thaw cycles. We verified that resistant cells cultured in drug-free media for a long time also persisted their resistance to vincristine. However, we observed that resistant cells cultured in vincristine-containing media continuously better maintained their resistance to vincristine when compared to culturing resistant cells in drug-free media (**Figure 23**). Since maintaining the resistance phenotype is critical for the consistency of experiments that will be performed with these resistant subpopulations, we recommend that newly established resistant cells should be cultured in drug-containing media to fully maintain their resistant to vincristine.

To examine the mechanism of vincristine resistance we checked the relative expression of some MDR associated genes, namely ABCB1, ABCC1, ABCG2 and LRP, between parental and resistant cells at first. As shown in **Figure 22**, newly established vincristine-resistant cells increased the expression of MDR associated genes such as ABCC1, ABCG2 and LRP. Although P-glycoprotein, encoded by ABCB1, is the main drug efflux protein associated with vincristine resistance, we could not determine the relative ABCB1 mRNA expression between parental and resistant cells most likely due to its very low expression in DAOY cells. To better reveal the mechanism of vincristine-resistance, the response of resistant cells to vincristine upon ABCB1, ABCC1, ABCG2, and LRP loss should be examined. To further investigate the mechanism of vincristine resistance, we will perform RNA-sequencing of parental and resistant cells as well.

It has been revealed that MLL2 and its binding partner KDM6A (trithorax group proteins, trxG) function together to activate gene expression during normal development. MLL2 methylates histone at the fourth lysine residue (H3K4me) while KDM6A acts as a H3K27me3

demethylase. The increase in active H3K4me3 marks and the removal of H3K27me3 repressive residues result in the activation of gene expression[71]. On the other hand, Polycomb (PcG) group proteins have the antagonistic function to TrxG proteins by repressing gene transcription via accumulation of H3K27me3 repressive marks[90]. It has been identified that the balance between H3K4 and H3K27 methylation is disrupted in Group 3 and Group 4 medulloblastomas due to inactivating mutations of MLL2, KDM6A and KDM6B and overexpression of the EZH2 (H3K27 methyltransferase). These aberrations result in a H3K27me3-enriched phenotype in Group 3 and Group 4 subgroups, which are the most aggressive subtypes of medulloblastoma[71]. Since the role of histone demethylases in medulloblastoma and how H3K27me3-enriched phenotype contributes the aggressiveness of Group 3 and Group 4 medulloblastomas are ill-defined, we focused on the functions of KDM6A and KDM6B at first. Initially, we examined whether KDM6A and KDM6B loss affect the medulloblastoma cell proliferation by using three different approaches. Both trypan exclusion assay and xCELLigence real-time cell analysis revealed that KDM6A or KDM6B loss did not change medulloblastoma cell growth. As both KDM6A and KDM6B are H3K27 demethylases, we hypothesized that loss-of-function of one of these genes might be compensated by the other one. Therefore, we targeted KDM6A and KDM6B at the same time by specific shRNAs and examined the proliferation rate of dual knockdown cells by flow cytometry. The same number of KDM6A/KDM6B dual knockdown cells tagged with green fluorescent protein (GFP) and non-tagged shControl cells were co-cultured for 9 days and the change in the amount of GFP+ cell was determined every 3 days by flow cytometry. Although we observed a significant increase in the proliferation of shKDM6A/6B cells within three days, the proliferation rate of shKDM6A/6B and shControl cells were similar at the end of nine days. These results imply that there could be other mechanisms contributing the aggressiveness of Group 3 and Group 4 tumors. Firstly, it has been revealed that H3K27me3 mark represses the expression of lineage-specific genes and maintains stem cells at the undifferentiated state[68]. Generally, cancer stem cells are more resistant to drugs compared to other cell types and they can repopulate the tumor, resulting in therapy resistance. Therefore, we speculate that inactivation of KDM6A/6B and subsequent enrichment in H3K27me3 marks may contribute the aggressiveness of medulloblastoma cells through keeping them stem like-state. To this end, the expression of stem cell markers such as CD133, CD15, Bmi1, Musashi1, Sox2, Sox9, and Nestin[91] should be determined upon KDM6A/6B loss to better reveal the role of H3K27me3 enriched phenotype on the aggressiveness of MB cells. Secondly, the knockdown efficiencies of shRNAs targeting KDM6A and KDM6B were low (around 40%) and possibly we are missing the phenotype due to low knockdown efficiencies. To this end, we will perform all these proliferation assays with new sets of shRNAs targeting KDM6A and KDM6B more efficiently. We will reveal the knockdown efficiency from protein levels by western bot and from mRNA

levels by RT-PCR. Once we targeted both KDM6A and KDM6B efficiently, we will repeat cell proliferation assays to investigate the role of KDM6A/6B loss on medulloblastoma cell growth. Finally, we will conduct RNA-sequencing to reveal the genome-wide transcriptome changes upon KDM6A/6B loss and GSK-J4 treatment, allowing us to identify the molecular players associated with aggressive MB subgroups.

To explore whether there are any connections between KDM6A/KDM6B loss and therapy resistance in medulloblastoma, we checked the response of KDM6A/KDM6B knockdown cells to vincristine. As shown in **Figure 28**, IC50s of vincristine were similar in KDM6A/KDM6B knockdown cells and non-transduced control cells, suggesting there were not strong correlation between KDM6A/KDM6B status and vincristine-resistance. Given that the epigenetic modifications may require some time to fully show their effects, we should repeat this experiment after subculturing KDM6A/KDM6B knockdown cells for a long time to better examine the effects of KDM6A/6B loss in vincristine-resistance. Also, knockdown efficiencies of both KDM6A and KDM6B at mRNA and protein levels should be verified in advance.

Our drug screen in parental and vincristine-resistant cells revealed that single treatments of potent HDAC6 inhibitors Tubastatin A and Rocilinostat reduced cell viability of parental DAOY cells while they were not effective in vincristine-resistant cells. HDAC6 deacetylates alpha-tubulin and acetylated alpha-tubulin is associated with stabilized microtubules[92]. It has been demonstrated that SHH driven medulloblastoma cells, including DAOY, showed increased expression of HDAC6 and inhibition of HDAC6 in SHH-medulloblastomas resulted in decreased cell viability, supporting our drug screen result[93]. Cancer cells have ability to develop resistance to microtubule destabilizing agents via several mechanisms. At this point we consider that generation of vincristine resistance in DAOY cells involves the altered expression of HDAC6. Most probably, resistant cells deregulated their epigenetic machinery and decreased the expression of HDAC6, allowing them to enhance microtubule stability by increasing acetylated tubulin level. Accordingly, unlike to parental cells, resistant cells that preferentially express low level of HDAC6 were not affected by inhibition of HDAC6 upon Tubastatin A and Rocilinostat treatments. To prove our hypothesis, we will determine the relative expression of HDAC6 in parental and vincristine-resistant cells at first and examine Tubastatin A and Rocilinostat response of these cells upon genetic inhibition of HDAC6 by shRNA or CRISPR/Cas9. Also, we will investigate whether overexpression of HDAC6 in resistant cells could revert the phenotype, resulting in increased sensitivity to Tubastatin A and Rocilinostat.

Finally, we performed drug combination screens both in parental and vincristine-resistant cells to discover potential compounds that induce cell death in medulloblastoma cells and that could be used in overcoming vincristine-resistance. From those, a single treatment of

Trichostatin A, 5-Iodotubercidin, IOX-1, CDX101, MAZ1805, Belinostat, KDOBA67, SGI-1776, Romidepsin, PCI-24781, Mocetinostat and MAZ1392 induced cell death both in parental and resistant cells significantly, revealing their potential to overcome vincristine resistance. In addition, we discovered that combined treatment of A-395, CBP/BRD4, GSK-J5, GSK343, GSK864, LLY-507, OF-1, SGC-CBP30, SRT1720 and UNC2400 with vincristine (50 nM) promoted cell death compared to vincristine alone treatments. Most importantly, we identified that single treatment of bromodomain inhibitors, namely CBP/BRD4, OF-1 and SGC-CBP30, did not induce cell death in medulloblastoma cells; however, they were highly effective in combination with vincristine. As inactive compounds such as GSK-J5 and UNC2400 also emerged as hits in our drug combination screen, we should validate our screen results at first. Once these combinations are validated, we will combine these epigenetic inhibitors with vincristine in different concentrations and calculate the combination index (CI), allowing us to understand whether these combinations are pharmacodynamically synergistic or additive. Testing these drug combinations in different concentrations is critical to discover novel efficacious combinations to overcome vincristine-resistance in medulloblastoma cells.

To identify the essential epigenetic modifiers playing role in the generation and maintenance of acquired vincristine-resistance in MB cells, we focused on compounds emerged as hits when they are combined with vincristine. We revealed that different classes of epigenetic probes such as bromodomain inhibitors (CBP/BRD4, OF-1 and SGC-CBP30), histone methyltransferase inhibitors (LLY-507, GSK343), histone deacetylase inhibitor (SRT1720), PCR2 complex inhibitor (A-395) and mutant IDH1 inhibitor (GSK864) could revert resistant phenotype when they were combined with vincristine, suggesting that the mechanism of acquired vincristine-resistance involves the deregulation of epigenetic machinery over time. Our suggested mechanism for vincristine-resistance was shown in **Figure 34**. A tumor contains a small number of tumour-sustaining cells and abundant tumor bulk cells. Upon vincristine treatment, a rare population of tumor cells that undergone epigenetic modulation can survive. However, vincristine tolerance is reversible at this epigenetically poised state. Drug removal results in reversal of poised state and it will lead to generation of drug-sensitive clonal derivatives. On the contrary, further exposure of poised cells to vincristine causes state transition, generating a drug-resistant population of tumor cells (resistant state). In our case, we think that treatment of vincristine resulted in epigenetic deregulation in parental cells, enabling them to survive in the presence of vincristine (epigenetically poised state). Afterwards, continuous treatment of vincristine allowed these cells to regulate their epigenetic machinery further, resulting in the generation of resistant populations. Particularly, we determined that targeting bromodomain family proteins namely CBP, BRD4, EP300 and BRPF with different epigenetic inhibitors resulted in reversion of resistant state to sensitive state,

suggesting that vincristine-resistant cells become dependent on the activity of these epigenetic modifiers to maintain their resistant phenotype. To uncover the critical molecular players during epigenetic state transition, the response of resistant cells to vincristine should be further examined upon genetic loss of candidate genes. As we also determined that vincristine-resistant cells showed increased expression of MDR genes, we will examine whether these bromodomain family proteins play role in the altered expression of MDR genes associated with vincristine resistance.

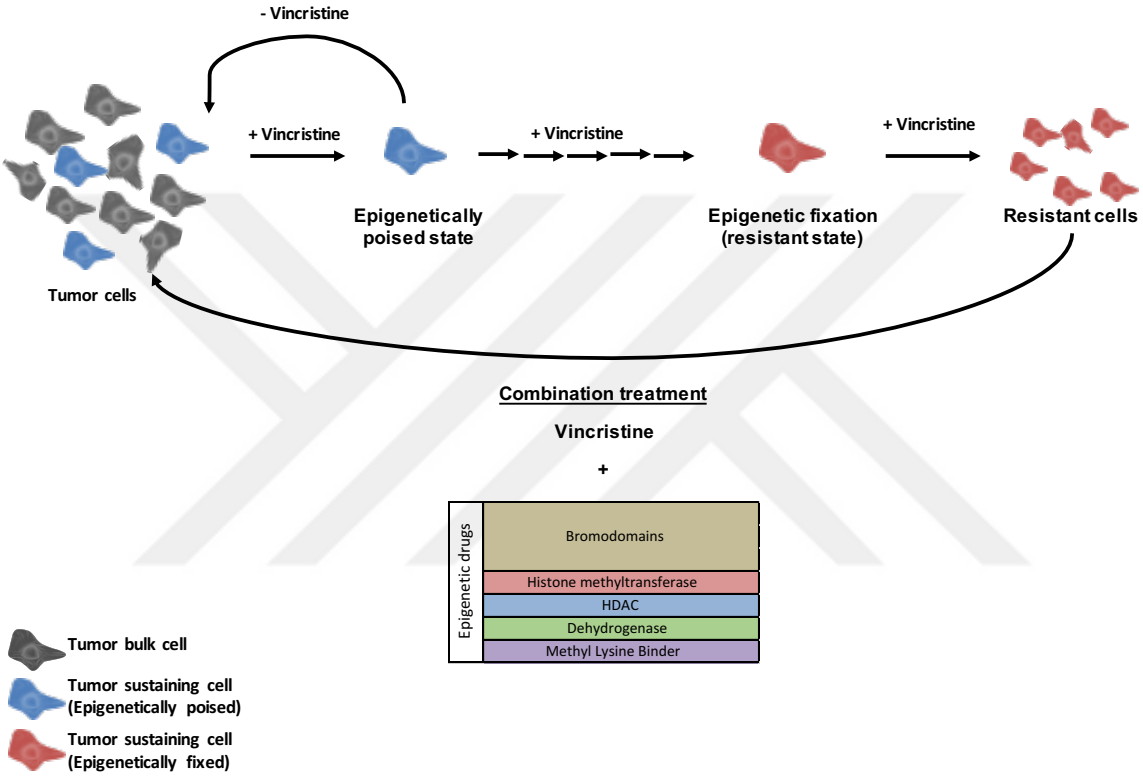

Figure 34. Suggested mechanism of acquired vincristine-resistance and how to overcome it by combination treatments.

Taken together, our results suggest that combination treatment of epigenetic drugs and vincristine can revert epigenetic state transition, finally resulting in generation of drug-sensitive cells.

In conclusion, our results suggest that targeting chromatin modifying enzymes can be a promising therapeutic approach for medulloblastoma treatment. Also, our results reveal the effectiveness of combination treatment of epigenetic inhibitors and chemotherapeutic agents to overcome therapy resistance in medulloblastoma

REFERENCES

1. Archer TC, Pomeroy SL. Medulloblastoma biology in the post-genomic era. *Futur Oncol*. 2012;8(12):1597-1604. doi:10.2217/fon.12.151.

2. Taylor MD, Northcott PA, Korshunov A, et al. Molecular subgroups of medulloblastoma: The current consensus. *Acta Neuropathol*. 2012;123(4):465-472. doi:10.1007/s00401-011-0922-z.

3. Louis DN, Perry A, Reifenberger G, et al. The 2016 World Health Organization Classification of Tumors of the Central Nervous System: a summary. *Acta Neuropathol*. 2016;131(6):803-820. doi:10.1007/s00401-016-1545-1.

4. Kool M, Korshunov A, Remke M, et al. Molecular subgroups of medulloblastoma: An international meta-analysis of transcriptome, genetic aberrations, and clinical data of WNT, SHH, Group 3, and Group 4 medulloblastomas. *Acta Neuropathol*. 2012;123(4):473-484. doi:10.1007/s00401-012-0958-8.

5. Packer RJ, Gajjar A, Vezina G, et al. Phase III Study of Craniospinal Radiation Therapy Followed by Adjuvant Chemotherapy for Newly Diagnosed Average-Risk Medulloblastoma. *J Clin Oncol*. 2006;24(25):4202-4208. doi:10.1200/JCO.2006.06.4980.

6. Rutkowski S, Bode U, Deinlein F, et al. Treatment of Early Childhood Medulloblastoma by Postoperative Chemotherapy Alone. *N Engl J Med*. 2005;352(10):978-986. doi:10.1056/NEJMoa042176.

7. Gajjar A, Chintagumpala M, Ashley D, et al. Risk-adapted craniospinal radiotherapy followed by high-dose chemotherapy and stem-cell rescue in children with newly diagnosed medulloblastoma (St Jude Medulloblastoma-96): long-term results from a prospective, multicentre trial. *Lancet Oncol*. 2006;7(10):813-820. doi:10.1016/S1470-2045(06)70867-1.

8. Mabbott DJ, Spiegler BJ, Greenberg ML, Rutka JT, Hyder DJ, Bouffet E. Serial evaluation of academic and behavioral outcome after treatment with cranial radiation in childhood. *J Clin Oncol*. 2005;23(10):2256-2263. doi:10.1200/JCO.2005.01.158.

9. Mabbott DJ, Penkman L, Witol A, Strother D, Bouffet E. Core neurocognitive functions in children treated for posterior fossa tumors. *Neuropsychology*. 2008;22(2):159-168. doi:10.1037/0894-4105.22.2.159.

10. Spiegler BJ, Bouffet E, Greenberg ML, Rutka JT, Mabbott DJ. Change in

Neurocognitive Functioning After Treatment With Cranial Radiation in Childhood. *J Clin Oncol*. 2004;22(4):706-713. doi:10.1200/JCO.2004.05.186.

11. Clifford SC, Lusher ME, Lindsey JC, et al. Wnt/Wingless Pathway Activation and Chromosome 6 Loss Characterise a Distinct Molecular Sub-Group of Medulloblastomas Associated with a Favourable Prognosis. *Cell Cycle*. 2006;5(22):2666-2670. doi:10.4161/cc.5.22.3446.

12. Thompson MC, Fuller C, Hogg TL, et al. Genomics identifies medulloblastoma subgroups that are enriched for specific genetic alterations. *J Clin Oncol*. 2006;24(12):1924-1931. doi:10.1200/JCO.2005.04.4974.

13. Li Q, Zhang P, Zhang C, et al. DDX3X regulates cell survival and cell cycle during mouse early embryonic development. *J Biomed Res*. 2014;28(4):282-291. doi:10.7555/JBR.27.20130047.

14. Robinson G, Parker M, Kranenburg T a, et al. Novel mutations target distinct subgroups of medulloblastoma. *Nature*. 2012;488(7409):43-48. doi:10.1038/nature11213.

15. Ellison DW, Onilude OE, Lindsey JC, et al. β-Catenin Status Predicts a Favorable Outcome in Childhood Medulloblastoma: The United Kingdom Children's Cancer Study Group Brain Tumour Committee. *J Clin Oncol*. 2005;23(31):7951-7957. doi:10.1200/JCO.2005.01.5479.

16. Gibson P, Tong Y, Robinson G, et al. Subtypes of medulloblastoma have distinct developmental origins. *Nature*. 2010;468(7327):1095-1099. doi:10.1038/nature09587.

17. Goodrich L V, Milenković L, Higgins KM, Scott MP. Altered neural cell fates and medulloblastoma in mouse patched mutants. *Science*. 1997;277(5329):1109-1113. http://www.ncbi.nlm.nih.gov/pubmed/9262482. Accessed July 8, 2017.

18. Jones DT, Jager N, Kool M, et al. Dissecting the genomic complexity underlying medulloblastoma. *Nature*. 2012;488(7409):100-105. doi:10.1038/nature11284.

19. Pugh TJ, Weeraratne SD, Archer TC, et al. Medulloblastoma exome sequencing uncovers subtype-specific somatic mutations. *Nature*. 2012;488(7409):106-110. doi:10.1038/nature11329.

20. Northcott PA, Shih DJH, Peacock J, et al. Subgroup-specific structural variation across 1,000 medulloblastoma genomes. *Nature*. 2012;488(7409):49-56. doi:10.1038/nature11327.

21. Shih DJH, Northcott PA, Remke M, et al. Cytogenetic Prognostication Within

Medulloblastoma Subgroups. *J Clin Oncol*. 2014;32(9):886-896. doi:10.1200/JCO.2013.50.9539.

22. Northcott PA, Korshunov A, Pfister SM, Taylor MD. The clinical implications of medulloblastoma subgroups. *Nat Rev Neurol*. 2012;8(6):340-351. doi:10.1038/nrneurol.2012.78.

23. Gajjar AJ, Robinson GW. Medulloblastoma-translating discoveries from the bench to the bedside. *Nat Rev Clin Oncol*. 2014;11(12):714-722. doi:10.1038/nrclinonc.2014.181.

24. Gerber NU, Mynarek M, von Hoff K, Friedrich C, Resch A, Rutkowski S. Recent developments and current concepts in medulloblastoma. *Cancer Treat Rev*. 2014;40(3):356-365. doi:10.1016/j.ctrv.2013.11.010.

25. KIJIMA N, KANEMURA Y. Molecular Classification of Medulloblastoma. *Neurol Med Chir (Tokyo)*. 2016;56(11):687-697. doi:10.2176/nmc.ra.2016-0016.

26. Sirachainan N, Nuchprayoon I, Thanarattanakorn P, et al. Outcome of medulloblastoma in children treated with reduced-dose radiation therapy plus adjuvant chemotherapy. *J Clin Neurosci*. 2011;18(4):515-519. doi:10.1016/j.jocn.2010.08.012.

27. Makale MT, McDonald CR, Hattangadi-Gluth JA, Kesari S. Mechanisms of radiotherapy-associated cognitive disability in patients with brain tumours. *Nat Rev Neurol*. 2017;13(1):52-64. http://dx.doi.org/10.1038/nrneurol.2016.185.

28. Oyharcabal-Bourden V, Kalifa C, Gentet JC, et al. Standard-risk medulloblastoma treated by adjuvant chemotherapy followed by reduced-dose craniospinal radiation therapy: a French Society of Pediatric Oncology Study. *J Clin Oncol*. 2005;23(21):4726-4734. doi:10.1200/JCO.2005.00.760.

29. Packer R, Finlay J. Chemotherapy for Childhood Medulloblastoma and Primitive Neuroectodermal Tumors. *Oncologist*. 1996;1(6):381-393. http://www.ncbi.nlm.nih.gov/pubmed/10388020.

30. Moudi M, Go R, Yien CYS, Nazre M. Vinca Alkaloids. *Int J Prev Med*. 2013;4(11):1231-1235. http://www.ncbi.nlm.nih.gov/pmc/articles/PMC3883245/.

31. Jordan MA, Wilson L. Microtubules as a target for anticancer drugs. *Nat Rev Cancer*. 2004;4(4):253-265. doi:10.1038/nrc1317.

32. Wang D, Lippard SJ. Cellular processing of platinum anticancer drugs. *Nat Rev Drug Discov*. 2005;4(4):307-320. doi:10.1038/nrd1691.

33. Hande KR. Topoisomerase II inhibitors. *Update Cancer Ther*. 2008;3(1):13-26.

doi:10.1016/j.uct.2008.02.001.

34. Nitiss JL. DNA topoisomerase II and its growing repertoire of biological functions. *Nat Rev Cancer*. 2009;9(5):327-337. doi:10.1038/nrc2608.

35. Emadi A, Jones RJ, Brodsky RA. Cyclophosphamide and cancer: golden anniversary. *Nat Rev Clin Oncol*. 2009;6(11):638-647. doi:10.1038/nrclinonc.2009.146.

36. Larkin JMG, Hughes SA, Beirne DA, et al. A Phase I/II study of lomustine and temozolomide in patients with cerebral metastases from malignant melanoma. *Br J Cancer*. 2007;96(1):44-48. doi:10.1038/sj.bjc.6603503.

37. Wang J. DNA damage and apoptosis. *Cell Death Differ*. 2001;8(11):1047-1048. doi:10.1038/sj.cdd.4400938.

38. Tian H, Cronstein BN. Understanding the mechanisms of action of methotrexate: implications for the treatment of rheumatoid arthritis. *Bull NYU Hosp Jt Dis*. 2007;65(3):168-173. http://www.ncbi.nlm.nih.gov/pubmed/17922664. Accessed July 9, 2017.

39. Lori F, Lisziewicz J. Rationale for the Use of Hydroxyurea as an Anti-Human Immunodeficiency Virus Drug. *Clin Infect Dis*. 2000;30(Supplement 2):S193-S197. doi:10.1086/313851.

40. Packer RJ, Sutton LN, Elterman R, et al. Outcome for children with medulloblastoma treated with radiation and cisplatin, CCNU, and vincristine chemotherapy. *J Neurosurg*. 1994;81(5):690-698. doi:10.3171/jns.1994.81.5.0690.

41. Evans AE, Jenkin RD, Sposto R, et al. The treatment of medulloblastoma. Results of a prospective randomized trial of radiation therapy with and without CCNU, vincristine, and prednisone. *J Neurosurg*. 1990;72(4):572-582. doi:10.3171/jns.1990.72.4.0572.

42. Tait DM, Thornton-Jones H, Bloom HJ, Lemerle J, Morris-Jones P. Adjuvant chemotherapy for medulloblastoma: the first multi-centre control trial of the International Society of Paediatric Oncology (SIOP I). *Eur J Cancer*. 1990;26(4):464-469. http://www.ncbi.nlm.nih.gov/pubmed/2141512. Accessed July 11, 2017.

43. Bailey CC, Gnekow A, Wellek S, et al. Prospective randomised trial of chemotherapy given before radiotherapy in childhood medulloblastoma. International Society of Paediatric Oncology (SIOP) and the (German) Society of Paediatric Oncology (GPO): SIOP II. *Med Pediatr Oncol*. 1995;25(3):166-178. http://www.ncbi.nlm.nih.gov/pubmed/7623725. Accessed July 11, 2017.

44. Krischer JP, Ragab AH, Kun L, et al. Nitrogen mustard, vincristine, procarbazine, and

prednisone as adjuvant chemotherapy in the treatment of medulloblastoma. *J Neurosurg*. 1991;74(6):905-909. doi:10.3171/jns.1991.74.6.0905.

45. Geyer JR, Zeltzer PM, Boyett JM, et al. Survival of infants with primitive neuroectodermal tumors or malignant ependymomas of the CNS treated with eight drugs in 1 day: a report from the Childrens Cancer Group. *J Clin Oncol*. 1994;12(8):1607-1615. doi:10.1200/JCO.1994.12.8.1607.

46. Kunschner LJ, Kuttesch J, Hess K, Yung WK. Survival and recurrence factors in adult medulloblastoma: the M.D. Anderson Cancer Center experience from 1978 to 1998. *Neuro Oncol*. 2001;3(3):167-173. http://www.ncbi.nlm.nih.gov/pubmed/11465397. Accessed July 10, 2017.

47. Abacioglu U, Uzel O, Sengoz M, Turkan S, Ober A. Medulloblastoma in adults: treatment results and prognostic factors. *Int J Radiat Oncol Biol Phys*. 2002;54(3):855-860. http://www.ncbi.nlm.nih.gov/pubmed/12377339. Accessed July 11, 2017.

48. Friedrich C, von Bueren AO, von Hoff K, et al. Treatment of adult nonmetastatic medulloblastoma patients according to the paediatric HIT 2000 protocol: A prospective observational multicentre study. *Eur J Cancer*. 2013;49(4):893-903. doi:10.1016/j.ejca.2012.10.006.

49. Rao AAN, Wallace DJ, Billups C, Boyett JM, Gajjar A, Packer RJ. Cumulative cisplatin dose is not associated with event-free or overall survival in children with newly diagnosed average-risk medulloblastoma treated with cisplatin based adjuvant chemotherapy: Report from the Children's Oncology Group. *Pediatr Blood Cancer*. 2014;61(1):102-106. doi:10.1002/pbc.24670.

50. Holohan C, Schaeybroeck S Van, Longley DB, Johnston PG. Cancer drug resistance : an evolving paradigm. *Nat Publ Gr*. 2013;13(10):714-726. doi:10.1038/nrc3599.

51. Housman G, Byler S, Heerboth S, et al. Drug Resistance in Cancer: An Overview. *Cancers (Basel)*. 2014;6(3):1769-1792. doi:10.3390/cancers6031769.

52. Allis, C.D., Jenuwein, T., and Reinberg D. *Epigenetics*. Cold Spring Harbor, NY: Cold Spring Harbor Laboratory Press; 2007.

53. Berger SL, Kouzarides T, Shiekhattar R, Shilatifard A. An operational definition of epigenetics. *Genes Dev*. 2009;23(7):781-783. doi:10.1101/gad.1787609.

54. Dawson MA, Kouzarides T. Cancer epigenetics: From mechanism to therapy. *Cell*. 2012;150(1):12-27. doi:10.1016/j.cell.2012.06.013.

55. Portela A, Esteller M. Epigenetic modifications and human disease. *Nat Biotechnol*.

2010;28(10):1057-1068. doi:10.1038/nbt.1685.

56. Baylin SB, Jones PA. A decade of exploring the cancer epigenome — biological and translational implications. *Nat Rev Cancer*. 2011;11(10):726-734. doi:10.1038/nrc3130.

57. Robertson KD. DNA methylation and human disease. *Nat Rev Genet*. 2005;6(8):597-610. doi:10.1038/nrg1655.

58. Jurkowska RZ, Jurkowski TP, Jeltsch A. Structure and Function of Mammalian DNA Methyltransferases. *ChemBioChem*. 2011;12(2):206-222. doi:10.1002/cbic.201000195.

59. Li E, Bestor TH, Jaenisch R. Targeted mutation of the DNA methyltransferase gene results in embryonic lethality. *Cell*. 1992;69(6):915-926. http://www.ncbi.nlm.nih.gov/pubmed/1606615. Accessed July 7, 2017.

60. Okano M, Bell DW, Haber DA, Li E. DNA methyltransferases Dnmt3a and Dnmt3b are essential for de novo methylation and mammalian development. *Cell*. 1999;99(3):247-257. http://www.ncbi.nlm.nih.gov/pubmed/10555141. Accessed July 7, 2017.

61. Ley TJ, Ding L, Walter MJ, et al. DNMT3A Mutations in Acute Myeloid Leukemia. *N Engl J Med*. 2010;363(25):2424-2433. doi:10.1056/NEJMoa1005143.

62. Suvà ML, Riggi N, Bernstein BE. Epigenetic Reprogramming in Cancer. *Science (80-)*. 2013;339(6127). http://science.sciencemag.org/content/339/6127/1567. Accessed July 9, 2017.

63. Barski A, Cuddapah S, Cui K, et al. High-resolution profiling of histone methylations in the human genome. *Cell*. 2007;129(4):823-837. doi:10.1016/j.cell.2007.05.009.

64. Ropero S, Esteller M. The role of histone deacetylases (HDACs) in human cancer. *Mol Oncol*. 2007;1(1):19-25. doi:10.1016/j.molonc.2007.01.001.

65. Barneda-Zahonero B, Parra M. Histone deacetylases and cancer. *Mol Oncol*. 2012;6(6):579-589. doi:10.1016/j.molonc.2012.07.003.

66. Xhemalce B, Dawson MA, Bannister AJ, Xhemalce B, Dawson MA, Bannister AJ. Histone Modifications. In: *Encyclopedia of Molecular Cell Biology and Molecular Medicine*. Weinheim, Germany: Wiley-VCH Verlag GmbH & Co. KGaA; 2011. doi:10.1002/3527600906.mcb.201100004.

67. Hanahan D, Weinberg RA. Hallmarks of cancer: The next generation. *Cell*. 2011;144(5):646-674. doi:10.1016/j.cell.2011.02.013.

68. Northcott PA, Jones DTW, Kool M, et al. Medulloblastomics: the end of the beginning.

Nat Rev Cancer. 2012;12(12):818-834. doi:10.1038/nrc3410.

69. Northcott PA, Nakahara Y, Wu X, et al. Multiple recurrent genetic events converge on control of histone lysine methylation in medulloblastoma. *Nat Genet*. 2009;41(4):465-472. doi:10.1038/ng.336.

70. Mack SC, Hubert CG, Miller TE, Taylor MD, Rich JN. An epigenetic gateway to brain tumor cell identity. *Nat Neurosci*. 2015;19(1):10-19. doi:10.1038/nn.4190.

71. Dubuc AM, Remke M, Korshunov A, et al. Aberrant patterns of H3K4 and H3K27 histone lysine methylation occur across subgroups in medulloblastoma. *Acta Neuropathol*. 2013;125(3):373-384. doi:10.1007/s00401-012-1070-9.

72. Parsons DW, Li M, Zhang X, et al. The Genetic Landscape of the Childhood Cancer Medulloblastoma. *Science (80-)*. 2011;331(6016):435-439. doi:10.1126/science.1198056.

73. Skowron P, Ramaswamy V, Taylor MD. Genetic and molecular alterations across medulloblastoma subgroups. *J Mol Med (Berl)*. 2015;93(10):1075-1084. doi:10.1007/s00109-015-1333-8.

74. Justin N, Zhang Y, Tarricone C, et al. Structural basis of oncogenic histone H3K27M inhibition of human polycomb repressive complex 2. *Nat Commun*. 2016;7. doi:10.1038/ncomms11316.

75. Alimova I, Venkataraman S, Harris P, et al. Targeting the enhancer of zeste homologue 2 in medulloblastoma. *Int J Cancer*. 2012;131(8):1800-1809. doi:10.1002/ijc.27455.

76. Shi X, Wang Q, Gu J, Xuan Z, Wu JI. SMARCA4/Brg1 coordinates genetic and epigenetic networks underlying Shh-type medulloblastoma development. *Oncogene*. 2016;35(44):5746-5758. doi:10.1038/onc.2016.108.

77. CellTiter-Glo ® Luminescent Cell Viability Assay. https://worldwide.promega.com/-/media/files/resources/protocols/technical-bulletins/0/celltiter-glo-luminescent-cell-viability-assay-protocol.pdf?la=en. Accessed July 17, 2017.

78. Kroemer G, Galluzzi L, Vandenabeele P, et al. Classification of cell death: recommendations of the Nomenclature Committee on Cell Death 2009. *Cell Death Differ*. 2009;16(1):3-11. doi:10.1038/cdd.2008.150.

79. Nikoletopoulou V, Markaki M, Palikaras K, Tavernarakis N. Crosstalk between apoptosis, necrosis and autophagy. *Biochim Biophys Acta - Mol Cell Res*. 2013;1833(12):3448-3459. doi:10.1016/j.bbamcr.2013.06.001.

80. Holubec H, Payne CM, Bernstein H, et al. Assessment of Apoptosis by Immunohistochemical Markers Compared to Cellular Morphology in Ex Vivo–stressed Colonic Mucosa. *J Histochem J Histochem Cytochem Histochem Cytochem*. 2005;53(53). doi:10.1369/jhc.4A6386.2005.

81. Martin AM, Raabe E, Eberhart C, Cohen KJ. Management of pediatric and adult patients with medulloblastoma. *Curr Treat Options Oncol*. 2014;15(4):581-594. doi:10.1007/s11864-014-0306-4.

82. Louis DN, Perry A, Reifenberger G, et al. The 2016 World Health Organization Classification of Tumors of the Central Nervous System: a summary. *Acta Neuropathol*. 2016;131(6):803-820. doi:10.1007/s00401-016-1545-1.

83. Padovani L, André N, Constine LS, Muracciole X. Neurocognitive function after radiotherapy for paediatric brain tumours. *Nat Rev Neurol*. 2012;8(10):578-588. doi:10.1038/nrneurol.2012.182.

84. Hashizume R, Andor N, Ihara Y, et al. Pharmacologic inhibition of histone demethylation as a therapy for pediatric brainstem glioma. *Nat Med*. 2014;20(12):1394-1396. doi:10.1038/nm.3716.

85. Dubuc AM, Remke M, Korshunov A, et al. Aberrant patterns of H3K4 and H3K27 histone lysine methylation occur across subgroups in medulloblastoma. *Acta Neuropathol*. 2013;125(3):373-384. doi:10.1007/s00401-012-1070-9.

86. Heinemann B, Nielsen JM, Hudlebusch HR, et al. Inhibition of demethylases by GSK-J1/J4. *Nature*. 2014;514(7520):E1-E2. doi:10.1038/nature13688.

87. Ecker J, Oehme I, Mazitschek R, et al. Targeting class I histone deacetylase 2 in MYC amplified group 3 medulloblastoma. *Acta Neuropathol Commun*. 2015;3:22. doi:10.1186/s40478-015-0201-7.

88. Pei Y, Liu K-W, Wang J, et al. HDAC and PI3K Antagonists Cooperate to Inhibit Growth of MYC- Driven Medulloblastoma. *Cancer Cell*. 2016;29(3):311-323. doi:10.1016/j.ccell.2016.02.011.

89. Mcdermott M, Eustace AJ, Busschots S, et al. In vitro development of chemotherapy and targeted therapy drug-resistant cancer cell lines : a practical guide with case studies. 2014;4(March). doi:10.3389/fonc.2014.00040.

90. Schuettengruber B, Martinez A-M, Iovino N, Cavalli G. Trithorax group proteins: switching genes on and keeping them active. *Nat Rev Mol Cell Biol*. 2011;12(12):799-814. doi:10.1038/nrm3230.

91. Manoranjan B, Venugopal C, McFarlane N, et al. Medulloblastoma stem cells: where development and cancer cross pathways. *Pediatr Res*. 2012;71(4-2):516-522. http://dx.doi.org/10.1038/pr.2011.62.

92. Hubbert C, Guardiola A, Shao R, et al. HDAC6 is a microtubule-associated deacetylase. *Nature*. 2002;417(6887):455-458. doi:10.1038/417455a.

93. Dhanyamraju PK, Holz PS, Finkernagel F, Fendrich V, Lauth M. Histone Deacetylase 6 Represents a Novel Drug Target in the Oncogenic Hedgehog Signaling Pathway. doi:10.1158/1535-7163.MCT-14-0481.

VITA

Tolga Lokumcu was born in Artvin, Turkey in 1990. He attended Samsun Science High School between 2005 and 2009. In 2015, he received his Bachelor of Science degree in Molecular Biology and Genetics from Istanbul Technical University, Turkey. From 2015 to 2017, he attended Biomedical Sciences and Engineering Master of Science Program at Koç University as a research and teaching assistant. He will continue his PhD studies in DKFZ, Heidelberg, Germany.